General Disclaimer

One or more of the Following Statements may affect this Document

- This document has been reproduced from the best copy furnished by the organizational source. It is being released in the interest of making available as much information as possible.

- This document may contain data, which exceeds the sheet parameters. It was furnished in this condition by the organizational source and is the best copy available.

- This document may contain tone-on-tone or color graphs, charts and/or pictures, which have been reproduced in black and white.

- This document is paginated as submitted by the original source.

- Portions of this document are not fully legible due to the historical nature of some of the material. However, it is the best reproduction available from the original submission.

Produced by the NASA Center for Aerospace Information (CASI)

(NASA-TM-83989) THE ACCELERATION AND PROPAGATION OF SOLAR FLARE ENERGETIC PARTICLES (NASA) 85 p HC A05/MF A01 CSCL 03B

N83-29162

Unclas
G3/92 03979

NASA

Technical Memorandum 83989

The Acceleration and Propagation of Solar Flare Energetic Particles

M. A. Forman, R. Ramaty and E. G. Zweibel

AUGUST 1982

JUN 1983
RECEIVED
NASA STI FACILITY
ACCESS DEPT.

National Aeronautics and
Space Administration

Goddard Space Flight Center
Greenbelt, Maryland 20771

THE ACCELERATION AND PROPAGATION OF SOLAR FLARE ENERGETIC PARTICLES

M. A. Forman
Department of Earth and Space Sciences
State University of New York
Stony Brook, New York 11794

R. Ramaty
Laboratory for High Energy Astrophysics
Goddard Space Flight Center
Greenbelt, Maryland 20771

E. G. Zweibel
Department of Astro-Geophysics
University of Colorado
Boulder, Colorado 80309

Chapter 11 in "The Physics of the Sun"

Edited by
T. E. Holzer
D. Mihalas
P. A. Sturrock
R. K. Ulrich

TABLE OF CONTENTS

I. INTRODUCTION 4

II. ENERGETIC PARTICLES IN SOLAR FLARES 6

a. Electromagnetic Radiations 7
Radio Emissions 7
Hard X Rays 9
Gamma Rays 11

b. Energetic Particles 15
Energy Spectra and Electron-Proton Correlations 16
Chemical Compositions 20
Isotopic and Ionic Composition 23

III. MECHANISMS OF SOLAR FLARE PARTICLE ACCELERATION 25

a. Stochastic Acceleration 26

b. Shock Acceleration 37

c. Acceleration in Direct Electric Fields 45

IV. SOLAR FLARE PARTICLE ENERGY SPECTRA IN INTERPLANETARY SPACE 51

V. SUMMARY AND OUTLOOK 56

ORIGINAL PAGE IS
OF POOR QUALITY

ABSTRACT

Observations and theories of particle acceleration in solar flares are reviewed. The most direct signatures of particle acceleration in flares are gamma rays, X rays and radio emissions produced by the energetic particles in the solar atmosphere and energetic particles detected in interplanetary space and in the Earth's atmosphere. We discuss the implication of these observations, we review the theories of stochastic and shock acceleration as well as acceleration in direct electric fields, and we briefly discuss interplanetary particle propagation. We attempt to present an overview of the highlights of both current and promising future research.

ORIGINAL PAGE IS
OF POOR QUALITY

I. INTRODUCTION

Acceleration of energetic particles is a wide spread phenomenon in nature, one that occurs at a variety of sites ranging from the Earth's magnetosphere to distant objects such as supernovae, active galaxies and quasars. There are in fact many explosive phenomena in astrophysics, solar flares among them, in which energetic particles are routinely produced and often contain a large fraction of all the available energy.

It is widely believed (e.g. Syrovatskii 1981) that solar flares draw their energy from the annihilation of magnetic fields. The strong electric fields which accompany such annihilation should accelerate particles, and in addition the rapid energy deposition following the annihilation should be an important source of shocks and turbulence. As proposed by Fermi (1949), charged particles can be accelerated to high energies in repeated reflections from magnetized clouds, or, in the more recent view, from hydromagnetic turbulence and shocks. This mechanism must be important in solar flares where shocks are known to exist and turbulence is expected to be produced by both shocks and other mechanisms.

Because the Sun is close to the Earth, particle acceleration in flares can be observed in considerable detail. The relevant observables are electromagnetic radiations produced by the accelerated particles in the solar atmosphere and energetic particles that escape from the Sun and are directly detected in interplanetary space. From the analysis of electromagnetic radiations and energetic particles observed from flares it follows that not all solar flare particles species are accelerated to their final energies at the same time. There appears to be a first-phase particle acceleration which produces mostly non-relativistic electrons and a second phase which accelerates ions and relativistic electrons. It is not clear, however,

ORIGINAL PAGE IS
OF POOR QUALITY

whether these two phases are manifestations of different acceleration mechanisms, or whether they are due to the evolution in space and time of the same mechanism modified by different energy loss and particle transport processes. Also, recent gamma-ray observations have shown that energetic ions can be produced very promptly, within a few seconds of the nonrelativistic electrons.

The energy spectrum resulting from solar flare particle acceleration can be determined down to a few MeV/nucleon from the maximum flux at each energy as observed in interplanetary space. This spectrum is clearly not a power law; simple shock and stochastic acceleration models appear to produce energy spectra that can fit the data. The chemical composition of solar energetic ions observed in interplanetary space, while grossly similar to the composition of the solar atmosphere, varies from one flare to another, and occasionally departs dramatically from the photospheric composition. These variations probably result from the existence of acceleration thresholds and injection mechanisms which depend on the charge and mass of the particles. The ionic states of energetic particles give some indication that the particles observed in interplanetary space are accelerated in the corona; they also seem to imply that selective heating mechanisms are occasionally important.

We review the observations and their implications in Section II, we treat acceleration by turbulence, by shocks, and in direct electric fields in Section III, we discuss the problem of the determination of solar flare particle energy spectra from interplanetary observations in Section IV, and we summarize the paper and provide an outlook for future research in Section V.

ORIGINAL PAGE IS
OF POOR QUALITY

II. ENERGETIC PARTICLES IN SOLAR FLARES

The solar flare is capable of producing a rich and complex particle population characterized by a broad spectrum of particle energies and containing many different chemical, isotopic and ionic species. Of these, the most commonly accelerated particles are electrons of energies in the range from about 10 to 100 keV. Information on these particles is obtained from hard X-ray observations (e.g. Hudson 1979, Kane et al. 1980), from microwave and Type III radio observations (e.g. Lin 1974), and from direct electron detections in interplanetary space (e.g. Lin 1974, Ramaty et al. 1980).

Solar flares also accelerate protons, nuclei and relativistic electrons. The nucleonic component is observed in interplanetary space (e.g. McDonald, Fichtel and Fisk 1974), it is occasionally detected on the ground by neutron monitors (e.g. Shea and Smart 1973, Duggal 1979) and its interactions at the Sun are manifest in gamma-ray lines (Chupp et al. 1973, Ramaty, Kozlovsky and Lingenfelter 1975, Chupp 1982). Relativistic electrons are observed directly in interplanetary space (Simnett 1971, Datlowe 1971, Evenson, Meyer and Yanagita 1981) and their interactions at the Sun produce gamma-ray continuum (Suri et al. 1975) and Type IV radio emission (e.g. Ramaty et al. 1980).

In the present Section we review the most pertinent data on solar energetic particles and discuss their implications. Electromagnetic emissions are discussed in IIa and the direct particle observations are in IIb. Since much of the information on solar radio emission is treated in a separate article in this volume (Smith and Goldman 1982), we discuss this topic only briefly here. Solar hard X-ray observations have also been reviewed in considerable detail recently (Hudson 1979, Kane et al. 1980) as have been the

ORIGINAL PAGE IS
OF POOR QUALITY

gamma-ray observations (Ramaty 1982, in this volume).

a. Electromagnetic Radiations

The electromagnetic emissions that contain the least ambiguous information on solar energetic particles are radio emissions, X-rays and gamma-rays. Other emission such as EUV and white light radiations are not discussed in the present article, but the reader can refer to other recent reviews (e.g. Kane et al. 1980, Ramaty et al. 1980).

It has been known for sometime (Wild, Smerd and Weiss 1963, Frost and Dennis 1971, Lin 1974, Ramaty et al. 1980) that at least two phases of particle acceleration can occur in solar flares. The first phase is characterized by impulsive bursts of hard X-rays and microwaves and by Type III radio emission, while the second phase is manifest in Type II bursts, microwave and metric Type IV emission, flare continuum radio emission and gradual hard X-rays. Gamma-ray emission is probably due to particles accelerated in both the first and second phases. The first phase has typical rise times of seconds or less and durations as short as a few seconds, while the second phase, in general, has longer rise times and durations. We proceed now to discuss these emissions in more detail.

Radio Emissions

As just mentioned, first-phase acceleration in the radio band is characterized by impulsive microwave bursts and Type III radio bursts. Impulsive microwave bursts are generally believed to be due to gyrosynchrotron radiation of electrons of energies in the range from several tens to several hundreds of keV (Takakura 1960, Ramaty 1969). Type III bursts result from the conversion into electromagnetic emission of Langmuir waves excited by beams of electrons of energies in the 10 to 100 keV range (Wild, Smerd amd Weiss

ORIGINAL PAGE IS
OF POOR QUALITY

1963). The same energy electrons also produce hard X-rays (see below). These electrons have access to both closed field lines of low loops, where they radiate microwaves and hard X-rays, and open field lines where they produce type III bursts. The electrons on open field lines can also be directly observed in interplanetary space (e.g. Lin 1974).

Second phase acceleration is characterized by Type II radio bursts, microwave Type IV bursts, flare continuum and moving Type IV emission. Type II bursts, presumably also due to the conversion of Langmuir waves, are indicators of shock fronts (Wild, Smerd and Weiss 1963) in the corona. Particle acceleration by these shocks, or by the turbulence behind them, is consistent with many second-phase phenomena including the protons and nuclei observed in interplanetary space. This conclusion is based on the good correlation between proton events and Type II bursts (Svestka and Fritzova 1974). The Type II emission itself is probably produced by 10 to 100 keV electrons that are also accelerated by the shock.

Type IV emission, in general, is due to gyrosynchrotron radiation of relativistic electrons. This emission includes microwave Type IV bursts, produced in low coronal loops where the magnetic field is relatively high, and moving Type IV bursts which are generally observed in the corona. The microwave Type IV emission can be distinguished from impulsive microwave bursts by their delayed rise to maximum intensity. The moving Type IV bursts are due to synchrotron radiation of ~ 1 MeV electrons in coronal magnetic fields of a few gauss. Flare continuum emission is also observed in the corona at the time of the passage of a Type II burst. As opposed to moving Type IV bursts, this emission is stationary and is believed to be due to plasma radiation (Dulk, Melrose and Smerd 1978).

ORIGINAL PAGE IS
OF POOR QUALITY

Hard X-Rays

Hard X-rays in solar flares result from the bremsstrahlung of electrons in the energy range from about 10 to several hundred keV. In the X-ray band, first-phase acceleration is characterized by impulsive hard X-ray bursts. The correlation between these bursts and impulsive microwave bursts (e.g. Lin 1974) indicates that both emissions should be produced by essentially the same electron population. As already mentioned, these electrons also produce Type III radio bursts. The first-phase mechanism is thought to be responsible for the impulsive acceleration of 10 to several hundred keV electrons in flares (e.g. Ramaty et al. 1980).

The most detailed information on first phase acceleration of electrons comes from hard X-ray observations. This information, however, is model dependent. Two limiting cases exist regarding the nature of the electrons. They could belong to a nonthermal population whose number density is lower than that of the relatively cool ambient medium with which it interacts, or they could form a quasithermal hot plasma. In the former case, the radiation yield is the ratio of the bremsstrahlung production rate to the nonradiative collisional loss rate. Since in the X-ray band this yield is very small ($\sim 10^{-5}$ at 25 keV), hard X-ray production in flares should be accompanied by the deposition of large amounts of energy into the solar atmosphere. On the other hand, in thermal models (Chubb 1970, Crannell et al. 1978), a larger fraction of the electron energy content could in principle be emitted as hard X-rays. But it turns out that it is difficult to confine the hot electrons to dense regions for times comparable to their radiation loss time (Smith and Auer 1980) and therefore the radiation yield of the thermal models is probably not much higher than that of the non-thermal one.

There are also a variety of particle interaction models which can be

crudely classified as thin- or thick-target (e.g. Kane et al. 1980). In the thin-target model (Datlowe and Lin 1973) the X-rays are produced by electrons which escape from the interaction region at the Sun, while in the thick-target model (Brown 1971, Hudson 1972), X-ray production takes place as the electrons slow down in the solar atmosphere. Clearly, the radiation yield is lower for a thin-target than for a thick-target, because for the latter, in addition to the collisional losses, the electrons also carry away kinetic energy. However, from the comparison of number of electrons observed in interplanetary space with that needed to produce the impulsive hard X-rays at the Sun, it follows (Lin 1974) that the majority of the 10 to 100 keV electrons remain trapped at the Sun and produce X-rays in thick-target interactions.

Various estimates exist of the energies deposited in the solar atmosphere by electrons accelerated in the first phase. From the summary of Ramaty et al. (1980) we have that in the thick-target and nonthermal model, the energy deposited by electrons above 25 keV is $\sim 2\times10^{32}$ ergs for the August 4, 1972 flare, which was one of the strongest events observed. The energy deposited in other cases ranges from about 5 to 50×10^{29} ergs in typical strong events, and from about 2 to 20×10^{28} ergs in typical small events. The fact that these energies are comparable to the total observed flare energies has led to the suggestion (Lin and Hudson 1976) that most flare phenomena could be accounted for, at least energetically, by the interaction of the first-phase electrons with the solar atmosphere.

First-phase acceleration must be very efficient, both in the amount of energy that it converts into accelerated particle energy, as we have just seen, and the number of ambient particles that it accelerates. The mechanism, however, accelerates fewer protons to 10 to 100 keV than electrons, as indicated by the absence of nonthermal wings of hydrogen Lyα (Canfield and

Cook 1978). We discuss below the recent gamma-ray evidence for the impulsive acceleration of MeV protons. As we shall see, the energy content in these particles is also lower than that in the 10 to 100 keV electrons. Mechanisms for first-phase acceleration have been reviewed by Smith (1979).

In addition to the impulsive component, solar hard X-rays occasionally exhibit a gradual component (duration ~ 10 minutes) which is believed to be a manifestation of second-phase acceleration. Hudson (1979) has reviewed the evidence for this component. It can be found in hard X-ray observations from flares located behind the limb of the Sun (Hudson, Lin and Stewart 1981) and from flares on the visible solar hemisphere which produce extended X-ray bursts (Frost and Dennis 1971, Hoyng, Brown and Van Beek 1976). These X-rays are produced in the corona and their spectrum is generally harder than that of the impulsive X-rays. This indicates additional acceleration. But the energy deposited in the solar atmosphere by the 10 to 100 keV electrons responsible for the gradual X-rays is lower by at least an order of magnitude than that deposited by the electrons of the impulsive phase (Hudson 1979).

Gamma-Rays

Gamma-ray lines, produced in energetic particle reactions in the solar atmosphere (Ramaty, Kozlovsky and Lingenfelter 1975), are tracers of the nucleonic component accelerated in flares. Many narrow and broad lines are produced (e.g. Ramaty, Kozlovsky and Lingenfelter 1979). The strongest narrow line is at 2.22 MeV from neutron capture on hydrogen. This line has been seen from a number of flares so far, as have some of the other strong narrow lines, e.g. at 4.44 MeV from ^{12}C, at 6.13 MeV from ^{16}O and at 0.51 MeV from positron annihilation (Chupp 1982, Ramaty 1982, in this volume). In addition to being observed individually, nuclear lines make a significant contribution to the total gamma-ray emission above 1 MeV (Ramaty et al. 1980). In particular, in

ORIGINAL PAGE IS
OF POOR QUALITY

the 4 to 7 MeV band, nuclear radiation appears to be the dominant emission mechanism (Ramaty, Kozlovsky and Suri 1977, Ibragimov and Kocharov 1977). On the other hand, gamma-ray emission up to an MeV is almost entirely due to electron bremsstrahlung and hence is a good tracer of the relativistic electrons in this energy range. Nuclear reactions in the solar atmosphere occasionally produce high energy neutrons which can travel as far as the Earth resulting in detectable neutron fluxes (Lingenfelter and Ramaty 1967). High energy neutrons were observed from a large flare in 1980 (Chupp et al. 1982).

Gamma-ray observations can provide information on the timing of the acceleration of protons, nuclei and relativistic electrons, they can determine the energy deposited by the nucleonic component in the solar atmosphere, and they can place constraints on the energy spectra of the protons and nuclei. Through Doppler shifts, gamma-ray lines could provide unique information on the beaming of the energetic particles (Ramaty and Crannell 1976, Kozlovsky and Ramaty 1977, Zweibel and Haber 1982).

We first address the question of the timing of the nucleonic acceleration and its relationship to the timing of the acceleration of the 10 to 100 keV electrons in the first phase. This question was studied (Bai and Ramaty 1976, Lin and Hudson 1976) for the August 4, 1972 flare which was the first flare from which nuclear gamma-rays were seen (Chupp et al. 1973).

The time dependences of hard X-rays, gamma-ray continuum, high frequency microwave emission and the 2.22 MeV line for the August 4, 1972 flare are shown in Figure 1 (from Bai and Ramaty 1976). As can be seen, the emissions produced by relativistic electrons (> 0.35 MeV gamma-ray continuum and high-frequency microwave emission) had a time history different from that of the X-ray emission produced by < 100 keV electrons. This difference is manifest in that the gamma-ray continuum and microwave emission reached peak

ORIGINAL PAGE IS
OF POOR QUALITY

strength a few minutes later than the X-rays. In addition, as can be seen from Figure 1, the time profile of the 2.22 MeV line could be better explained when the time profile of neutron production was assumed to be similar to the time profile of the gamma-ray continuum rather than that of the X-rays. (See article by Ramaty 1982, in this volume, for a detailed discussion on the delay of the emission of 2.22 MeV photons owing to the finite capture time of the neutrons). This led Bai and Ramaty (1976) to conclude that the > 0.35 MeV electrons and > 10 MeV protons are accelerated in the second phase. However, as can be seen in Figure 1, even though the build-up of the higher energy emissions in the August 4, 1972 flare was slower than that of the hard X-rays, the two emissions were not clearly separated in time.

As opposed to the gradual build-up of the nucleonic component on a time scale of a few minutes seen in the August 4 event, the recent SMM (Chupp 1982) and HEAO-3 (Prince et al. 1982) observations have provided examples of very prompt acceleration of protons and nuclei. The most useful information in this regard comes from the comparison of the time history of the prompt gamma rays in the energy band from 4 to 7 MeV (which is dominated by nuclear gamma-rays) with that of the hard X-rays. For the June 7, 1980 flare (Chupp 1982) this comparison (Bai 1982) implies that the < 100 keV electrons and > 10 MeV nuclei were accelerated in very close time proximity (less than a few seconds). There are, nevertheless, differences between the two time profiles: there is a delay of approximately 2 sec between individual hard X-ray and gamma-ray peaks, and the gamma rays reach maximum strength at least 10 seconds after the X-rays. The small but finite lag of gamma rays behind the hard X-rays in the June 7 flare would be yet another manifestation of a second acceleration phase. This type of second-phase acceleration, i.e. one which is very closely correlated with the first-phase acceleration, has been

ORIGINAL PAGE IS
OF POOR QUALITY

referred to as second-step acceleration (Bai and Ramaty 1979, Bai 1982).

We next discuss the energy content in the nucleonic component and its relationship to the energy deposited by electrons accelerated in the first phase. The nucleonic energy content is the sum of the energy deposited during gamma-ray line production and the energy carried away by particles escaping from the Sun.

We consider numerical values for two flares (August 4, 1972 and June 7, 1980) for which the gamma-ray data have been analysed in considerable detail. These are given in Table 1. Here W_d (>1MeV/nucleon) and W_{esc} (>1MeV/nucleon) are, respectively, the energies deposited and carried away by the nucleonic component, W_e (>20keV) is the energy deposited by electrons above 20 keV, and $\bar{N}_p$ (>10 MeV) and $N_{esc,p}$ (>10 MeV) are the numbers of protons above 10 MeV that interact and escape from the Sun, respectively. For the August 4 flare, W_d and $\bar{N}_p$ are from Ramaty (1982, in this volume), W_{esc} and $N_{esc,p}$ are from Lin and Hudson (1976) and W_e has been given earlier in this section. For the June 7 flare, W_d and $\bar{N}_p$ are again from Ramaty (1982, in this volume), W_{esc} and $N_{esc,p}$ are from Von Rosenvinge, Ramaty and Reames (1981) and W_e is from A. Kiplinger (private communication 1981).

Considering the numerical values of Table 1, we first note that the escape conditions for the nucleonic component can vary considerably from one flare to another. While for the June 7 flare only a small fraction of the particles escaped from the Sun, for the August 4 flare the number of protons observed in space exceeded the number that interacted at the Sun by more than an order of magnitude. Evidently, in certain cases particles have access to open field lines while in others they do not. In both cases, however, the total energy in the nucleonic component is less than the energy deposited by the electrons accelerated in the first phase. Shocks, turbulence, or both.

ORIGINAL PAGE IS
OF POOR QUALITY

produced during energy deposition in the first phase, could thus be responsible for second-phase acceleration.

The gamma-ray observations also set constraints on the energy spectra of the protons and nuclei. The derived energy spectra (Ramaty 1982, in this volume) turn out to be consistent with those obtained from direct particle observations in interplanetary space (McGuire, Von Rosenvinge and McDonald 1981 and IIb). This agreement implies that the same acceleration mechanism could be responsible for both the escaping and trapped nucleonic component, even though the ratio between the numbers of particles in these two populations can vary dramatically from flare to flare. On the other hand we cannot rule out the possibility that these two populations are produced by different mechanisms.

For a discussion of additional implications of the solar gamma-ray observations (e.g. beaming, photospheric ^{3}He abundance, limb darkening effects) the reader is referred to the article by Ramaty (1982, in this volume.

b. Energetic Particles

Complementary to the electromagnetic radiations discussed in the previous subsection are the direct particle observations in interplanetary space and in the Earth's atmosphere. Spacecraft observations (e.g. Van Hollebeke 1979, Gloeckler 1979) can determine the energy spectra of the various particle species including electrons, the abundances of essentially all elements from H through Ni, and isotopic and ionic abundances for a few abundant elements. Ground based neutron monitor observations (e.g. Duggal 1979) extend the spectrum of the nucleonic component of solar flare particles to about 20 GeV. Particle observations, however, can only provide limited information on the timing of the acceleration. We proceed now to discuss the most pertinent

ORIGINAL PAGE IS
OF POOR QUALITY

of these observations.

Energy Spectra and Electron-Proton Correlations

Detailed studies of solar flare proton spectra that attempted to eliminate the effects of coronal and interplanetary transport were made by Bryant et al. (1965), Reinhard and Wibberenz (1974) and Van Hollebeke, Ma Sung and McDonald (1975). In the study of Van Hollebeke et al. the effects of propagation on the observed spectra were minimized by considering only particle events from flares that were well connected magnetically to the observing spacecraft and by constructing the proton energy spectra at times of maximum intensity at each energy (see Section IV). Because of instrumental limitations, however, the resultant energy spectra extended only over the narrow energy range from 20 to 80 MeV and therefore could not differentiate between various possible spectral fits such as power laws or exponentials.

A more recent study (McGuire, Von Rosenvinge and McDonald 1981) has extended considerably the particle energy range under investigation (1 to 400 MeV for protons) and has provided data on α-particle spectra as well. By using the same techniques for minimizing the propagation effects as Van Hollebeke et al. (1975), McGuire et al. (1981) find two spectral forms that provide good fits to the data. These are the Bessel function spectrum (Ramaty 1979, Section IIIa)

$$\frac{dJ}{dE}(E) \propto \beta K_2[2(3\beta/\alpha T)^{1/2}] \quad , \tag{1}$$

and an exponential spectrum in rigidity

$$\frac{dJ}{dE}(E) \propto \exp(-R/R_0)\, dR/dE. \tag{2}$$

ORIGINAL PAGE IS
OF POOR QUALITY

Here dJ/dE is differential intensity measured in particles/(cm^2sec sr MeV/nucleon), $v = c\beta$, E and R are particle velocity, energy per nucleon and rigidity, respectively, and K_2 is the modified Bessel function of order 2 (Abramowitz and Stegun 1966). The parameters αT for the Bessel function and R_0 for the exponential characterize the shape of the particle energy spectra. Equation (1) was shown to be the solution of a transport equation for stochastic acceleration with acceleration efficiency α and loss time T (M. A. Lee private communication 1978, Ramaty 1979, Section IIIa).

An example of the results of McGuire et al. (1981) is shown in Figure 2. Here the data points show the observed particle intensities from the November 5, 1974 event, and the solid and dashed curves are given by equations (1) and (2), respectively. The spectral parameters for this event are αT = 0.024 and R_0 = 73 MV for protons, and αT = 0.015 and R_0 = 80 MV for α particles. A very important result of McGuire et al. (1981) is that power laws in energy ($dJ(E)/dE \propto E^{-\gamma}$ with γ a constant) do not fit the data over the entire observed energy range, as can be clearly seen from Figure 2.

The variability of the spectral parameters αT and R_0 from one flare to another was also studied by McGuire et al. (1981). They find, as did Van Hollebeke et al. (1975) before, that for the well-connected flares the spectral parameters are confined to rather narrow ranges. For protons, αT = 0.025 ± 0.011 and R_0 = 70 ± 27 MV. The α-particlespectra are generally steeper than the proton spectra. The ratios of the proton to α-particle αT's and R_0's are 1.6 ± 0.2 and 0.7 ± 0.1, respectively (R. McGuire, private communication 1981).

We pointed out in IIa that constraints on the energy spectra of the protons and nuclei that interact at the Sun can be set by gamma-ray line ratio observations. Unlike the interplanetary observations, these data are not

ORIGINAL PAGE IS
OF POOR QUALITY

influenced by propagation effects, but they depend on the assumed interaction model. For thick-target interactions, Ramaty (1982, in this volume) finds that for 7 flares for which line ratios are available, αT (assumed to be the same for all particle species) is in the range 0.014 to 0.020. This relatively narrow range is consistent with that found by McGuire et al. (1981) from interplanetary observations. As already mentioned, the implication of this result is that a single mechanism could be responsible for both the escaping and trapped nucleonic component.

We turn now to a discussion of electron energy spectra and correlations between electrons and protons of various energies. Energy spectra of electrons accelerated in solar flares were analysed by Lin (1971, 1974) and recently by Lin, Mewaldt and Van Hollebeke (1982) who have minimized the propagation effects in the same fashion as was done for the protons and α particles discussed above. An energy spectrum of a large electron event is shown in Figure 3 (from Lin, Mewaldt and Van Hollebeke 1982). The break at ~ 100 keV, characteristic of all solar flare electron spectra, is probably due to the acceleration process itself (Lin et al. 1982), since the time of maximum treatment is expected to minimize the propagation effects, and Coulomb losses in the solar atmosphere would produce a continuous flattening rather than a single break. For small electron events the energy spectra are steeper than the spectrum of Figure 3, both below and above the break. Whereas in large events, relativistic electrons are occasionally seen above 10 MeV (Datlowe 1971), in small events, electrons cannot be seen above a few hundred keV.

Correlations between electrons and protons were studied by Ramaty et al. (1980) and more recently by Evenson, Meyer and Yanagita (1981). Figure 4 (from Ramaty et al. 1980) shows the correlation between 0.5 to 1.1 MeV

ORIGINAL PAGE IS
OF POOR QUALITY

electrons and 10 MeV protons. As can be seen, for large events the two populations are well correlated, but for smaller events there is an overabundance of electrons. This effect is possibly a manifestation of the two acceleration phases, with the first-phase producing more electrons than protons in small events. The good correlation seen for larger events indicates that relativistic electrons just below an MeV and ~ 10 MeV protons could be accelerated by the same mechanism. This could be second-phase acceleration. The correlation between these two particle population is supported by the gamma-ray data. As discussed in IIa and seen in Figure 1, the >0.35 MeV continuum produced predominantly by <1 MeV electrons, and nuclear gamma rays from $\gtrsim$ 10 MeV protons, have similar time histories.

Evenson et al. (1981) have recently examined the relationship between protons and relativistic electrons at nearly the same energy (~ 10 MeV). They find that these two particle populations are very poorly correlated. In particular, the majority of the proton events have very low ($\lesssim 10^{-3}$) electron-to-proton ratios at ~ 10 MeV. This is in contrast to the correlation seen in Figure 4 where all proton events are accompanied by 0.5 to 1.1 MeV electrons. A few of the events, however, show larger electron-to-proton ratios, and some of them are as high as 0.2 at 10 MeV. Gamma rays (lines or continuum) were seen from all of these events. But it is not clear at the present time whether these electron enrichments are caused by the acceleration mechanism or whether they reflect different escape condition for protons and electrons. Oppositely directed beams of ions and electrons produced in a direct electric field could yield gamma-ray lines at the Sun and relativistic electrons in space. Such electric fields are discussed in Section IIIc.

Chemical Compositions

Nuclei heavier than He in solar energetic particles were first detected by Fichtel and Guss (1961) and since then many measurements of such particles have been made (see reviews by McDonald, Fichtel and Fisk 1974, Fan, Gloeckler and Hovestadt 1975, Ramaty et al. 1980). While the earlier results indicated rough agreement of the energetic particle composition with photospheric composition (e.g. Bertsch, Fichtel and Reames 1969), with more recent results, it became obvious that these two sets of abundances can differ drastically from each other.

The first indications for large abundance anomalies in flare accelerated particles came from the observations of Price et al. (1971) which showed large enhancements at low energies of iron-group nuclei over photospheric abundances. Further studies (Mogro-Campero and Simpson 1972, Teegarden, Von Rosenvinge and McDonald 1973) have revealed such enhancements also for Mg and Si.

The most dramatic departure of a solar energetic particle abundance from its photospheric value is that of ^{3}He (Garrard, Stone and Vogt 1973). Here very large enhancements are occasionally observed in the ^{3}He/^{4}He ratio above its likely photospheric value (see Ramaty et al. 1980 for a review of the data).

Enrichments of ^{3}He in energetic particle populations (for example, the galactic cosmic rays) have been generally attributed to nuclear reactions between the energetic particles and the ambient medium. But, as first pointed out by Garrard, Stone and Vogt (1973), this interpretation of the solar ^{3}He enrichments, in its simplest form, is inconsistent with much of the ^{3}He data. If the ^{3}He enrichments are due to nuclear reactions of the energetic particles, then they should be accompanied by similar enrichments in ^{2}H and,

to a lesser degree, in ^3H. Such enrichments, however, are not observed.

Several schemes based on nuclear reactions have been proposed to overcome this difficulty. These rely on the kinematics and angular distributions of the reaction products which favor the preferential escape of ^3He (Ramaty and Kozlovsky 1974, Rothwell 1976) and the thermonuclear destruction of ^2H and ^3H in a model in which the energetic products of the nuclear reactions are confined to thin filaments and interact with each other (Colgate, Audouze and Fowler 1977). But, as proposed by Fisk (1978) and Kocharov and Kocharov (1978), the enhanced ^3He abundance in solar energetic particles could be due to preferential heating of ambient ^3He. Provided that the acceleration mechanism has an injection threshold (Section III), such heating would greatly enhance the number of accelerated particles.

Several systematic studies of solar energetic particle composition have been carried out recently (McGuire, Von Rosenvinge and McDonald 1979, Cook, Stone and Vogt 1980, Mason et al. 1980, Reames and Von Rosenvinge 1981). The results of these studies are summarized in Figure 5. Here ratios of energetic particle abundances to photospheric abundances are shown for a variety of elements as well as for ^3He and ^4He.

For each element or isotope plotted in Figure 5 we consider flares for which the energetic particles are rich in ^3He and flares from which no ^3He is observed. The data for these two groups are separated by the dashed vertical lines, with ^3He-rich flares to the right of the lines and flares with no ^3He to their left.

The closed circles are the data of McGuire, Von Rosenvinge and McDonald (1979) who measured the energetic particle composition of eight large non ^3He-rich solar flares in the energy range from 6.7 to 15 MeV/nucleon. Such compositions were also measured by Cook, Stone and Vogt (1980) from a few to

15 MeV/nucleon and by Mason et al. (1980) near 1 MeV/nucleon. The values given by crosses and stars are the average particle abundances measured by Cook et al. (1980) and Mason et al. (1980), respectively, for their sample of large solar flares. As can be seen, these averages are consistent with the data of McGuire et al. (1979).

To the right of the dashed lines are data for ^{3}He-rich flares. The open circles represent the recent data of Reames and Von Rosenvinge (1981) for six flares, while the values given by the diamonds represent abundances labelled by Mason et al. (1980) as anomalous. In particular, diamond-1 is for their carbon-poor flares and diamond-2 is for the October 12-13, 1977 flares. Both these sets of energetic particles are rich in ^{3}He.

The distinction between ^{3}He-rich and normal events follows mainly from the ^{3}He abundance itself. The ^{3}He/O ratio of the former exceeds the upper limits on this ratio for the latter by at least an order of magnitude. The other abundances, however, are not too different for the two classes of events. As can be seen in Figure 5, ^{3}He-rich events can be both rich or poor in H (see values of diamonds-1 and 2 for H), although it has been noticed (e.g. Ramaty et al. 1980) that ^{3}He-rich flares have on the average low ^{1}H/^{4}He ratios. It also follows from Figure 5 that ^{4}He and C tend to be somewhat suppressed in ^{3}He-rich events although it is not necessarily true that all ^{3}He rich events are C poor. The variability from event to event in ^{4}He, C and other elements is larger in ^{3}He-rich events than in normal events.

Both normal and ^{3}He-rich events show enrichments in heavy elements, although these are significantly larger for the ^{3}He-rich events. The abundance enhancements in Ca and Fe are in fact almost as large as those of ^{3}He. The correlation between ^{3}He and Fe enhancements in ^{3}He-rich events was first noticed by Anglin, Dietrich and Simpson (1977).

Various models have been proposed to account for these abundance variations. Meyer (1981) has pointed out that some of the less dramatic abundance variation could simply reflect coronal abundances which are different from those of the photosphere. Mullan and Levine (1981) suggested that differences in Coulomb energy losses (Section IIIa) of partially stripped heavy ions could lower the injection thresholds of these ions and hence increase the number of particles that are accelerated. Eichler (1979) has pointed out that in acceleration by shocks of finite widths (Section IIIb), partially stripped ions with large gyroradii could be preferentially accelerated because they are capable of sampling more of the compression at the shock. This assumes a rigidity dependent mean free path (Section IIIb) and that all ions have the same initial velocities. Axford (1982) points out that, aside from this effect, the shock may selectively heat ions of different mass-to-charge ratios by plasma processes, so that the ions will be injected in a manner which depends on this ratio. In Fisk's (1978) model (see also Mason et al. 1980), the electrostatic ion cyclotron waves which heat the ^{3}He also heat partially stripped heavy ions which have A/Z near 3 (e.g. $^{16}O^{+5}$, $^{56}Fe^{+17}$) by resonance with the second harmonic of the particle cyclotron frequency. Only mechanisms which can selectively preheat certain ions, such as the mechanisms of Fisk (1978) and Kochorov and Kocharov (1978), combined with injection thresholds which are large compared to the thermal speeds of the normal ions in the source, can explain the observed ^{3}He enhancements.

Isotopic and Ionic Compositions

In addition to the ^{3}He observations discussed above, the only elements whose isotopic abundances have been observed in solar energetic particles are Ne and Mg (Dietrich and Simpson 1979, 1981, Mewaldt et al. 1979, 1981). For Ne, it has been found that $^{22}Ne/^{20}Ne = 0.13 \pm 0.003$ and $^{21}Ne/^{22}Ne < 0.1$.

These abundances are consistent with those of Neon-A in meteorites (Podosek 1978) which is believed to represent the primordial Ne isotopic abundance at the time of the formation of the solar system. The isotopic abundances of Ne in the photosphere are not known. In the solar wind, the $^{22}Ne/^{20}Ne$ ratio of 0.07 ± 0.002 (Geiss 1973) is significantly lower than in the solar energetic particles. The origin of this discrepancy is not yet understood. But because the Mg isotopic abundances in solar energetic particles, $^{25}Mg/^{24}Mg$ = 0.14(+0.05, - 0.02), $^{26}Mg/^{24}Mg$ = 0.15 (+ 0.04, - 0.03) (Mewaldt et al. 1981) seem to be consistent with primordial solar system material, it is possible that Ne isotopic fractionation takes place in the solar wind. Mg isotopic abundances have not yet been measured in the solar wind and are not known in the photosphere.

The first measurements (Gloeckler et al. 1976) of the ionic states of solar energetic particles revealed a charge distribution consistent with that of a gas in ionization equilibrium at about 1 to 2×10^6K. Subsequent measurements (Sciambi et al. 1977) found that the charge states of C and O in several solar particle events essentially do not vary with energy (from 0.037 to 1 MeV per charge), in time and from event to event. These results are consistent with particles being accelerated in coronal material and traversing little material during and after their acceleration. The recent observation (Hovestadt et al. 1981) of singly charged He ions in solar energetic particles indicates that cooler material is also accelerated. This could be due to temperature inhomogeneities in the corona or the injection of chromospheric material into the acceleration region.

Measurements of charge states have important implications on the heating mechanisms discussed above for producing the ^3He and heavy element abundance anomalies. Ma Sung et al. (1981) find that $^{16}O^{+5}$ and $^{56}Fe^{+17}$ are indeed

present in a ^3He rich flare, as would be expected in Fisk's (1978) model. However, the existence of appreciable concentrations of such ions in the ambient medium, requires that particles be accelerated from regions spanning a broad range of temperatures ($4x10^5$ to $5x10^6$K).

Recently, Kleckler et al. (1982) have reported that the mean charge of Fe during events with large ^3He and Fe enrichments is significantly larger than the mean charge of Fe during flares of normal composition. Since the charge of Fe during normal events is not expected to be as high as +17, this result is consistent with the heating model of Fisk (1978) which preferentially enhances Fe^{+17}.

III. MECHANISMS OF SOLAR FLARE PARTICLE ACCELERATION

Based on the observations described in the previous Section, a solar flare acceleration mechanism or combination of mechanisms must fulfill the following requirements: the acceleration mechanism must be capable of imparting a large fraction of the available flare energy to energetic particles and it must be possible to accelerate a significant fraction of ambient particles; the dominant mechanism or the combination of mechanisms should be capable of producing the spatial and temporal evolution of the different energetic particle populations, in particular the rapid rise of the various electromagnetic emissions; the mechanisms must have acceleration thresholds, which, with appropriate injection or preacceleration mechanisms, are capable of accounting for the observed compositions and their variations; and the mechanisms must be able to produce particles with the observed energy spectra.

The observations also indicate that the occurence of solar flare ions in

space is associated with coronal shocks and by implication with turbulence produced by the shock. Therefore, it is reasonable to invoke stochastic acceleration and direct shock acceleration for solar flare ion production. On an even more basic level, solar flares are associated with the release of magnetic energy by the collapse and reconnection of magnetic fields, and these processes may generate large transient electric fields which could accelerate ions and electrons directly.

In subsection (a) we discuss stochastic acceleration and in subsection (b) we discuss shock acceleration with emphasis on recent ideas of diffusive shock acceleration. For both mechanisms we consider energy spectra, the problem of injection, and the acceleration times of the particles. In subsection (c) we briefly discuss magnetic reconnection and electric fields and their possible role in particle acceleration.

The results of subsections (a) and (b) are most relevant to ion acceleration in solar flares. The reader is referred to several recent reviews of first-phase electron acceleration (e.g. Smith 1979, Ramaty et al. 1980, Brown and Smith 1980). Our treatment of particle acceleration, as well as the treatments that we review, do not discuss the generation and decay of the shocks and turbulence, and do not, for the most part, take into account the effect of the accelerated particles on the turbulence or on the shocks which accelerate them. This important aspect of acceleration theory remains a subject for future research.

a. Stochastic Acceleration

Processes in turbulent plasmas which cause particles to change their energy in a random way with many increases and decreases in energy lead to stochastic acceleration. In the original stochastic Fermi mechanism (Fermi 1949), the process was reflection from randomly moving magnetized clouds.

Stochastic acceleration can also result from resonant pitch-angle scattering from Alfven waves with wavelength of the order of the particle gyroradius. To accelerate paticles these waves must propagate both parallel and anti-parallel to the average magnetic field (Skilling 1975). Other modes of stochastic acceleration, called magnetic pumping and transit-time damping, occur through interaction with magnetosonic waves whose wavelengths are much longer than the particle gyroradius (Kulsrud and Ferrari 1971, Melrose 1980, Achterberg 1981). These modes require additional pitch-angle scattering to keep the particles isotropic. Langmuir (plasma) waves or other electrostatic waves with phase velocities of the order of the particle speed will also accelerate particles stochastically (Melrose 1980).

When the random energy increments are small compared to the particle energy, stochastic acceleration results in a diffusive current in momentum space, $S_p = - D_{pp}\partial f/\partial p$, where p is the magnitude of the momentum, f(p) is the number of particles per unit volume in phase space and S_p is measured in cm^{-3} momentum $^{-2}sec^{-1}$. Particles injected at some momentum p_0 will diffuse in momentum to larger and smaller p. In terms of f, the differential particle intensity per unit energy per nucleon is given by $dJ/dE = A\ p^2 f$, where A is the nuclear mass number. Additional non-diffusive energy changes can be added to S_p,

$$S_p = - D_{pp} \frac{\partial f}{\partial p} + \frac{dp}{dt} f \ , \qquad (3)$$

where dp/dt represents convection in momentum space due to processes which change the energy of all particles (e.g. ionization or Coulomb losses).

The momentum diffusion coefficient D_{pp} depends on the nature of the stochastic process. If the process is hard sphere scattering with mean free

ORIGINAL PAGE IS
OF POOR QUALITY

path λ, then D_{pp} can be derived (Parker and Tidman 1958, M. A. Lee, private communication 1978) from the Boltzmann equation. This yields

$$D_{pp} = p^2(\delta V)^2/3v\lambda \quad , \tag{4}$$

where $(\delta V)^2$ is the mean square velocity of the scatterers and v the particle speed.

If the stochastic acceleration is due to resonant pitch-angle scattering from Alfven waves, the momentum diffusion coefficient obtained from quasi-linear theory is (Skilling 1975)

$$D_{pp} = \frac{2p^2 V_A{}^2}{v^2} \int \frac{D_+ D_-}{D_+ + D_-} d\mu \tag{5}$$

where V_A is the Alfven speed, $D_+(D_-)$ is the pitch-angle scattering coefficient due to forward (backward) propagating Alfven waves, and μ is the cosine of the particle pitch angle in the mean field. It is clear from this equation that there is no stochastic acceleration due to Alfven waves unless the waves propagate in both directions. This requirement occurs because the electric fields of Alfven waves in one direction can be Lorentz-transformed away and so cannot accelerate particles. For example, Alfven waves generated by the streaming of energetic particles (Wentzel 1969) propagate only in the direction of the streaming and hence do not accelerate the particles.

By comparing equations (4) and (5) we can define an effective mean free path for stochastic acceleration by Alfven waves, $\lambda^A = p^2 V_A^2/3vD_{pp}{}^A$. This λ^A is, in general, a function of particle rigidity which is determined by the power spectrum of the Alfven waves. Let $W_\pm(k)$ be the energy density per wave number k in waves propagating in the + or - directions. Then, from quasi-

ORIGINAL PAGE IS
OF POOR QUALITY

linear theory (Hasselmann and Wibberenz 1968, Jokipii 1971, Luhmann 1976),

$$D_{\pm}(\mu) = v(2\pi Ze/pc)^2 \, W_{\pm}(1/\mu r_c)(1-\mu^2)/|\mu|, \tag{6}$$

where Ze is the particle charge and r_c its gyroradius in the average magnetic field, B. For example, if $D_+ = D_-$ and $W_{(k)} \propto k^{n-2}$,

$$\lambda^A(R) = \frac{B^2 r_c^{\,2}}{96\pi^2 W(1/r_c)} \, (2-n)\,(4-n) \propto R^n. \tag{7}$$

For stochastic acceleration due to long-wavelength magnetosonic waves (assuming adequate particle pitch-angle scattering) the expression for D_{pp} from quasi-linear theory is

$$D_{pp}^{\;M} = \xi \, \frac{p^2 V_A^{\,2}}{3v} \, \frac{\langle \delta B^2 \rangle}{B^2} \, \langle k \rangle \tag{8}$$

(adapted from Achterberg 1981), where $\langle \delta B^2 \rangle$ is the mean square of the fluctuations in the field magnitude and $\langle k \rangle$ is the mean wavenumber of the magnetosonic waves. The number ξ depends on the angular distribution of the waves and it is usually assumed that $\xi \sim 1$. Note that the λ^M corresponding to equation (7) is $B^2 \langle k \rangle^{-1} / \langle \delta B^2 \rangle$ and is independent of particle momentum or charge. It is not necessary for the magnetosonic waves to propagate in both directions to accelerate particles, but as already mentioned a certain level of pitch-angle scattering is required to isotropize the particles. This condition is $D_+ + D_- > D_{pp}^{\;M}/p^2$ (Achterberg 1981). Unlike for acceleration by Alfven waves, the waves which do this scattering are not required to propagate in both the + and - directions.

ORIGINAL PAGE IS
OF POOR QUALITY

The relative importance of acceleration by magnetosonic and by Alfven waves is given by $D_{pp}{}^{M}/D_{pp}{}^{A}$. In order of magnitude, this ratio is

$$\frac{D_{pp}{}^{M}}{D_{pp}{}^{A}} \sim \langle k \rangle\, r_c W^M \left(\frac{1}{k_r W_+(k_r)} + \frac{1}{k_r W_-(k_r)}\right) , \tag{9}$$

where $k_r = r_c^{-1}$ is the resonant wave number and W^M is the total energy density in the long wavelength magnetosonic waves. Since by assumption $\langle k \rangle r_c \ll 1$, acceleration by Alfven waves dominates when their energy density is comparable to that in magnetosonic waves, but only when there is appreciable power in Alfven waves propagating in both directions.

The momentum diffusion coefficient for isotropic Langmuir turbulence, $D_{pp}{}^{L}$, is given by Melrose (1980; e.q. 8.13). This results in a $\lambda^L \propto (A/Z)^2$ times a function of particle velocity.

The acceleration models which we now discuss in detail consider the physical mode of stochastic acceleration only through the momentum diffusion coefficient D_{pp}. Neglecting spatial convection, averaging over some volume of space and introducting an escape time T from this volume, particle conservation results in the transport equation

$$\frac{\partial f}{\partial t} + \frac{1}{p^2}\frac{\partial}{\partial p}(p^2 S_p) + \frac{f}{T} = Q(p,t) , \tag{10}$$

where Q(p,t) is the particle source in momentum space. Equation (10) has been applied to the acceleration of solar energetic particles by Barbosa (1979), Ramaty and Lee (Ramaty 1979) and Mullan (1980).

In Barbosa's (1979) model (hereafter referred to as model B) the acceleration is by Alfven waves with a power law spectrum for W(k), T is assumed to be a power law in velocity, $T \propto v^m$, and dp/dt is neglected. In

Mullan's model (1980, referred to as model M), the scattering is from neutral sheets in turbulent motion leading to a constant λ; numerical integration is used in order to incorporate realistic losses due to Coulomb scattering and adiabatic deceleration in an expanding turbulent region, followed by an energy-independent escape. The Ramaty-Lee model (Ramaty 1979, model RL) is a special case of the other two, since it assumes that both the mean free path and escape time are energy-independent and that dp/dt is negligible when acceleration is effective. These are rather special assumptions which need to be physically justified. Nevertheless, the predicted energy spectrum of this model fits the interplanetary observations of proton and α-particle spectra at 1AU very well (see Section IIb). Because of this and because of its inherent simplicity, we proceed to first discuss the RL model.

With a steady source of q particles/cm^{3}sec at momentum p_0, equation (10) becomes

$$\frac{\partial f}{\partial t} - \frac{1}{p^2}\frac{\partial}{\partial p}\left(\alpha\frac{p^4}{3\beta}\frac{\partial f}{\partial p}\right) + \frac{f}{T} = \frac{q\delta(p-p_0)}{4\pi p_0^{\,2}} \quad , \tag{11}$$

where the acceleration parameter $\alpha = (\delta V)^2/\lambda c$. The steady-state solutions of this equation are characterized by the dimensionless, energy-independent constant αT. For ultrarelativistic particles

$$f = \frac{q\left(\frac{p}{p_0}\right)^{-3/2 \pm (9/4 + 3/\alpha T)^{1/2}}}{4\pi p_0^{\,3}\alpha\,(1 + 4/3\alpha T)^{1/2}} \quad , \tag{12}$$

where the plus sign applies to $p<p_0$ and the minus sign to $p>p_0$. For non-relativistic particles and $p>p_0$

$$f = \frac{6q}{4\pi p_0^2 mc\alpha} \frac{p_0}{p} I_2 \left(2(3p_0/mc\alpha T)^{1/2}\right) K_2\left(2(3p/mc\alpha T)^{1/2}\right) , \qquad (13)$$

where m is the ion mass, and I_2 and K_2 are the modified Bessel functions of order 2 (Abramowitz and Stegun 1966). The arguments of I_2 and K_2 are interchanged for $p<p_0$. The corresponding intensity per energy per nucleon is $dJ/dE = Ap^2 f$.

The spectrum of dJ/dE is not a power-law. It has an energy-dependent slope $\gamma(E) \equiv - d\ln(dJ/dE)/d\ln E$ which approaches zero at low energies. From the asymptotic expression for $K_2(x) \propto x^{-1/2}\exp(-x)$, we find that at energies $E \gg 3.26\ \alpha^2 T^2$ MeV/nucleon

$$\frac{dJ}{dE} \propto E^{3/8} \exp\left(-\left(E/(3.26(\alpha T)^2)\right)^{1/4}\right) . \qquad (14)$$

This spectrum steepens with increasing energy up to the fully relativistic domain where equation (12) applies and $\gamma(E) = (1/2)(9 + 12/\alpha T)^{1/2} - 1/2$.

As discussed in Section IIb, McGuire, et al. (1981) have found that equations (13) or (14) fit the spectra of protons and α-particles in interplanetary space quite well with αT around 0.025 for protons. Different values of αT, however, are required for these two particle species; in many events the values of αT which fit the helium spectra are less than those for

ORIGINAL PAGE IS
OF POOR QUALITY

protons. The solar energetic particle spectra, therefore are not strictly velocity-dependent as implied by a constant λ. The possibility of a rigidity dependent diffusion mean free path is considered in the model of Barbosa (1979) which we discuss next.

As already mentioned, the B model uses the quasi-linear theory of particle resonant scattering to evaluate D_{pp} from a given spectrum of Alfven waves. The steady state spectrum of non-relativistic particles in this model, with $\lambda \propto R^n$ (cf. equation 7) and $T \propto v^m$, is

$$\frac{dJ}{dE} \propto v^{(1+n/2)} K_\nu \left(\frac{1}{s} \left(\frac{3v\lambda}{V_A^2 T}\right)^{1/2}\right) \quad , \tag{15}$$

where $s = (n+1-m)/2>0$ and $\nu = (2-n)/2s$. By using the asymptotic expression for $K_\nu(x)$, equation (15) can be written as

$$\frac{dJ}{dE} \propto E^{(3+n+m)/8} \exp\left(-\left(\frac{A}{Z}\right)^{n/2} \left(\frac{E}{3.26K^2}\right)^{(1+n-m)/4}\right) \quad , \tag{16}$$

which is valid if the argument of the exponential is much larger than unity. The constant K in equation (16) for the B model is equivalent to αT in equation (14) for the RL model. For n = m = 0 equations (15) and (16) reduce to equations (13) and (14), respectively, i.e. the B model reduces to the RL model.

For n>0 equation (16) predicts α-particle spectra, which, when expressed as functions of energy per nucleon, are steeper than the proton spectra for

the same K. This feature of the B model, not present in the RL model, is qualitatively consistent with the observations, as discussed above. But the comparison of equation (16) with the solar flare proton spectra for a variety of m's and n's shows that the best fit is obtained for m = n = 0. Other values make the slope of the spectrum vary more rapidly with energy than observed. For example, if m = 0, we find that equation (16) fits the observed proton spectrum shown in Figure 2 only if $n \lesssim 0.1$. For such small values of n, the α-particle spectrum is only slightly steeper than the proton spectrum with the same K, while the observed proton and α-particle spectra shown in Figure 2 are considerably different. Thus, while the B model allows rigidity dependent spectra, the fit of the calculations to the data implies that this rigidity dependence is not very pronounced.

In the M model, the scattering elements are assumed to move with velocities δV of the order of shock velocities in the corona. Since λ is assumed to be energy independent D_{pp}, is given by the same expression as in the RL model, equation (4). The dp/dt term in equation (3), however, is taken into account. In particular a time dependent combination of Coulomb and adiabatic deceleration losses followed by energy independent escape is used. Because of this complexity, the resultant energy spectra can only be given graphically. They are approximately constant below 1 MeV/nucleon, very steep above 100 MeV/nucleon, and have $\gamma \sim 3$ at ~ 50 MeV/nucleon. This is in general agreement with observed spectra, although detailed comparisons over an extended energy range have not yet been made.

A very important question in all particle acceleration theories, including stochastic acceleration, is that of injection. We first note that the basic concept of stochastic acceleration assumes that the energy changes are small compared with the particle energy and therefore the particle

velocity must be much greater than δV. Furthermore, for resonant scattering, ions must have $v>V_A$ to scatter from Alfven waves and electrons must have $v>43V_A$ to scatter from whistlers (Melrose 1974).

An additional injection condition is set by the requirement that the systematic acceleration rate due to diffusion in momentum space be larger than the ionization and Coulomb energy loss rates of the particles. The systematic acceleration rate is (e.g. Ramaty 1979)

$$\left(\frac{dp}{dt}\right)_{acc} = (vp^2)^{-1} \frac{\partial}{\partial p} (vp^2 D_{pp}) \quad , \tag{17}$$

and for D_{pp} from equation (4)

$$\left(\frac{dE}{dt}\right)_{acc} = \frac{4\alpha}{3} (E(E + 2Mc^2))^{1/2} \tag{18}$$

Here M and E are the proton mass and kinetic energy per nucleon for nuclei, and the electron mass and kinetic energy for electrons.

Energy loss rates due to ionization in a neutral medium and Coulomb losses in a fully ionized medium were summarized by Ramaty (1979). These loss rates together with the systematic acceleration rates for nuclei and electrons (equation 18) are plotted in Figures 6 and 7 for neutral and ionized media, respectively. Particles can be accelerated only if the rate of systematic energy gain exceeds the rate of energy loss. Depending on the ratio of the acceleration efficiency, α, to the ambient density, n, the energy gain curve

may or may not intersect the energy loss curve. In the former case an injection mechanism is required which preaccelerates the particles to $E \sim E_0$, where E_0 is the energy where the two curves intersect.

The values of α/n indicated in Figures 6 and 7 were chosen such that E_0 for electrons is around 0.1 MeV, an energy at which there seems to be a transition from first phase to second phase acceleration (Section II). For protons, however, these α/n's are such that the systematic gain is larger that the loss at all energies, and in this case it is possible to accelerate ambient particles directly. However, stochastic acceleration still requires that the particle velocities be larger than δV. Assuming that δV is of the order of the Alfven velocity, the particles must be accelerated either from a high β plasma (β = particle pressure/magnetic pressure) or possibly from the non-thermal tail of a low-β plasma. Such non-thermal tails are observed in the solar wind (Ogilvie, Scudder and Olbert 1978, Scudder and Ogilvie 1979). If the Alfven speed is the threshold, then ^{3}He-rich events cannot originate in high-β plasmas.

The solar energetic particle abundances and their variability must be strongly dependent on the injection process as we have discussed in Section IIb. Injection questions have not yet been fully investigated and they remain outstanding problems for future research.

The acceleration time of stochastic acceleration can be studied from the time dependent solutions of equation (10). Such solutions were obtained in the RL model for impulsive injection of particles at $t = 0$ and $p = p_0$, with $T \to \infty$ and λ = const. In Figure 8 (from Ramaty 1979) we show the differential proton and electron number densities ($N(E) = 4\pi p^2 f/v$) at various times t after injection. As can be seen, in a given time, protons are accelerated to much higher energies than electrons. This result is the direct

consequence of the acceleration rates shown in Figures 6 and 7 which assume the same α for protons and electrons.

From the gamma-ray observations (Section IIa) it follows that in at least some flares protons and nuclei are accelerated to energies greater than 10 MeV/nucleon in about 1 sec. As can be seen from Figure 8, acceleration of a significant fraction of the protons to such energies requires that $\alpha\tau \sim 0.1$. Then if $t \approx 1$ sec, $\alpha \approx 0.1$ sec^{-1}. Because δV can probably not be greater than 3×10^8 cm/sec, λ must be less than 3×10^7cm. Since this value is 50 times the gyroradius of a 20 MeV proton in a 1 Gauss field, we could expect such short mean free paths in the strong turbulence of solar flares. But there is no direct observational evidence for such turbulence.

The characteristic acceleration time in the B model is of the same form as in the RL model. Barbosa (1979) estimates that the acceleration time to 10 MeV can be as short as $\sim$ 10 seconds. As above, this requires strong turbulence on scales 10^6cm. Mullan (1980), on the other hand, estimates from numerical solutions that the time to accelerate keV protons to $\sim$ 5 MeV is about an hour. This time is too long for the acceleration of the gamma-ray producing protons and nuclei, but it could be adequate for the acceleration of the solar flare particles observed in interplanetary space.

b) Shock Acceleration

Solar flare shocks propagate upward through the solar corona at speeds of about 500 to 2000 km/sec, as indicated by Type II radio bursts (Smith and Goldman 1982 and Section IIa), and laterally through the chromosphere where they are seen as Moreton waves (Uchida 1974). The occurence of solar energetic particles in space is strongly correlated with flares having Type II bursts (Svestka and Fritzova 1974). Flare shocks are observed to accelerate particles in interplanetary space (Richter and Keppler 1977), as are

co-rotating shocks (Barnes and Simpson 1976, McDonald et al. 1976) and planetary bow shocks (Asbridge, Bame and Strong 1968, Lin, Meng and Anderson 1974, Scholer et al. 1980, Zwickl et al. 1981). A flare shock can transport particles in an energy-independent manner through the corona until they escape onto open field lines. Shock acceleration has been recently reviewed by Toptygin (1980) and Axford (1982) and applied to solar flares by Achterberg and Norman (1980), Decker, Pesses and Armstrong (1981) and Lee and Fisk (1982). See also McDonald (1981) for review.

There are basically two types of shock acceleration: scatter-free, in which particles gain energy by reflection in a single shock encounter (Sonnerup 1973, Chen and Armstrong 1975, Pesses, Decker and Armstrong 1982) and diffusive, in which particles gain energy by repeated scattering between the converging plasmas on either side of the shock (e.g. Axford, Leer and Skadron 1977, Axford 1982). The scatter-free mechanism can enhance the particle energy by about an order of magnitude if the shock is nearly perpendicular (i.e. the magnetic field is nearly perpendicular to the shock normal), but in that case, only particles with speeds which are already much greater than the shock speed can be reflected. Further acceleration, however, requires multiple reflections. These are possible if there is particle scattering in the fluid flow or if the particles are trapped between converging shocks in a flare loop (Wentzel 1965).

Acceleration by diffusive scattering across the shock is a first order Fermi process, in the sense that every shock crossing results in an energy gain. It is in principle more efficient than stochastic acceleration because it derives energy directly from the compression of the flow at the shock. For this mechanism to be effective, however, there must be adequate particle scattering both upstream and downstream of the shock. The passage of the

shock is expected to generate turbulence downstream which will scatter the particles. Scattering upstream, however, is more problematic (Holman, Ionson and Scott 1979). Observations (Tsurutani and Rodriquez 1981) of interplantetary shocks and planetary bow shocks show that when they are nearly parallel there is a very turbulent foreshock region capable of scattering particles. Such a region could be produced by the accelerated particles themselves (Achterberg and Norman 1980, Lee 1982).

In the simplest example of a plane shock where the only losses are due to convection of the particles away from the shock downstream, the energetic particle density in phase space is given by a power law, $f \propto p^{-3V/\Delta V}$, where V is the shock speed and ΔV the discontinuity in the plasma speed at the shock. In terms of the compression ratio, r, at the shock, $V/\Delta V = r/(r-1)$. For a strong shock in a non-relativistic fluid, $r = 4$ and hence $f(p) \propto p^{-4}$. For weaker shocks, $4>r>1$ and therefore the power-law is steeper. Blandford and Ostriker (1980) have modeled cosmic-ray acceleration and propagation in the Galaxy on the basis of this result, including acceleration by shocks with a spectrum of compression ratios. They have been able to reproduce the observed cosmic-ray spectrum which approximates a power law over a wide range of energies.

Unlike galactic cosmic rays, solar flare particles do not have power-law spectra (e.g. Figure 2). In fact, none of the energetic particle populations which are observed to be accelerated by shocks in interplanetary space have power-law spectra. Diffusive shock acceleration produces such curved spectra rather than power laws when particle energy losses or escape losses are significant, or when the shock has a finite size or lifetime, compared to the natural scales of the shock acceleration. For example, diffusive escape losses from the finite bow shock of the Earth (Eichler 1981, Forman 1981b,

Ellison 1981a, Lee 1982) and adiabatic losses near interplanetary shocks (Fisk and Lee 1980, Forman 1981a) have been shown to reproduce the observed spectra quite well.

In the present subsection we describe the general methods used to obtain energetic particle spectra from shock acceleration, and provide a simple solution of the appropriate transport equation which provides a spectrum that fits the solar flare data quite well.

The transport equation which describes diffusive shock acceleration is similar to equation (10) without the stochastic acceleration term proportional to D_{pp}, but with additional terms due to convective transport, spatial diffusion and adiabatic compression of particles in the plasma flow. This equation is given by (Axford 1982)

$$\frac{\partial f}{\partial t} + \mathbf{V}\cdot\nabla f - \nabla\cdot(k\cdot\nabla f) - \frac{\nabla\cdot\mathbf{V}}{3}\, p\,\frac{\partial f}{\partial p} + \frac{f}{T} + \frac{1}{p^2}\frac{\partial}{\partial p}\left(p^2\left(\frac{dp}{dt}\right)f\right) = Q(p,r,t), \quad (19)$$

where f, T and dp/dt have been defined in connection with equation (10), $\mathbf{V}$ is the plasma velocity and k the spatial diffusion tensor which couples the energetic particles to the plasma converging at the shock. The terms containing $\mathbf{V}$ and k are essential for the description of acceleration across the shock front. The injected particles are explicitly introduced in equation (19) by the source term Q; the injection may also be treated as a boundary condition such that f approaches a given value f_0 far upstream. The losses due to particle escape can be treated via the escape time T, or as diffusive escape. In the latter case the scattering becomes negligible at a finite distance from the shock.

The usual method for deriving a steady-state $\left(\frac{\partial f}{\partial t} = 0\right)$ particle spectrum is to first solve equation (19) separately on each side of the shock and then

to match the two solutions at the shock by imposing boundary conditions. These conditions are that both the energetic particle density and the normal component of the spatial streaming ($S = -4\pi p^2(Vp\frac{\partial f}{\partial p} + k\cdot\nabla f)$) of these particles be continuous at the shock. Toptygin (1980) has shown that this is an appropriate approach even though equation (19) is not valid very close to the shock.

We present here a steady-state solution of equation (19) by assuming that dp/dt is negligible and T is constant (as in the RL model for stochastic acceleration), that only diffusion along the shock normal is important (hence k can be treated as a scalar), that the shock is an infinite plane at x = 0 and infinitely thin, and that the particles are steadily injected at the shock, i.e. $Q = q\,\delta(x)\delta(p-p_0)/(4\pi p_0^2)$ where q is measured in particles cm^{-2} sec^{-1}. For these conditions, the solution on either side of the shock is given by

ORIGINAL PAGE IS
OF POOR QUALITY

$$f(x,p) = f(0,p)\exp(-\beta_i|x|)\ , \tag{20}$$

where upstream

$$\beta_i = \beta_1 = (V + (V^2 + 4k_1/T)^{1/2})/2k_1 \tag{21}$$

and downstream

$$\beta_i = \beta_2 = (-(V - \Delta V) + ((V - \Delta V)^2 + 4k_2/T)^{1/2})/2k_2. \tag{22}$$

The streaming continuity at the shock gives the equation

ORIGINAL PAGE IS
OF POOR QUALITY

$$\Delta V \frac{p}{3} \frac{\partial f}{\partial p} (0,p) + (k_1\beta_1 + k_2\beta_2)\, f(0,p) = \frac{q\delta(p-p_o)}{4\pi p_o^{\,2}} \tag{23}$$

The exact non-relativistic solution of this equation is

$$f(0,p) = \frac{3q}{4\pi p_o^{\,3}\Delta V} \left(\frac{p}{p_o}\right)^{-3V/\Delta V} \exp\left(-3(VI_1 + (V - \Delta V)I_2)/\Delta V\right) , \tag{24}$$

where

$$I_i = (1+\eta_i)^{1/2} - 1 - \mathrm{ctnh}^{-1}\,(1+\eta_i)^{1/2} - \ln\,(\eta_i/4)^{1/2} , \tag{25}$$

with $\eta_i = 4\lambda_i p/(3mV_i^2T)$. Since $I_i \to 0$ for $\eta_i \to 0$, the distribution function is a power law for $v \ll 3V_i^2T/4\lambda_i$ with the same spectral index $(3V/\Delta V)$ as for the case of a plane shock with no losses. However, when v becomes comparable to the lower value of $3V_i^2T/4\lambda_i$, the shape of the spectrum is determined by the exponential term in equation (24). In other words, the spectrum is determined by the losses on the side of the shock where V_i^2/λ_i is lower. This is probably the upstream side.

Assuming for simplicity that V^2/λ is the same on both sides of the shock, and that $3V/\Delta V = 4$, as for a strong shock, the differential intensity per energy per nucleon, for $v \gg 3V^2T/4\lambda$, is

$$\frac{dJ}{dE} \propto E^{-1} \exp\left(-(E/(0.422(\alpha T)^2))^{1/4}\right), \tag{26}$$

where $\alpha T = V^2T/(\lambda c)$. Equation (26) for shock acceleration is quite similar to equation (10) for stochastic acceleration in the RL model. These two spectra are compared in Figure 9 using values of αT which fit typical data in

both cases. As can be seen, the difference between them is most pronounced at the lowest energies where the solar flare spectrum is unknown because of adiabatic energy losses in the interplanetary medium (Section IV).

As for stochastic acceleration, for shock acceleration as well, the question of injection is very important. Ionization and Coulomb energy losses to the ambient medium have the same role in determining injection conditions in shock acceleration as they do in stochastic acceleration. In addition, for diffusive shock acceleration, particles downstream must have sufficient velocity to overtake the shock. This is at least $(V - \Delta V)$ directed towards the shock, and increases as $\cos^{-2}\psi$, where ψ is the angle between the downstream field and the shock normal. The velocity $V-\Delta V$ is at least as great as V_A or δV, and with the additional $\cos^{-2}\psi$ factor, the threshold for shock acceleration is expected to be higher than for stochastic acceleration.

Another injection condition is set by the finite width of the shock which could depend on many parameters including the pressure of the accelerated particles. When this pressure is taken into account (Axford, Leer, and Skadron 1977, Eichler 1979, Drury and Volk 1981, Drury, Axford and Summers 1982) all or part of the velocity change ΔV is smoothed out over a length scale $\sim \bar{k}/V$, where $\bar{k}$ is the diffusion coefficient of the energetic particles averaged over their energy spectrum. As pointed out in Section IIb, this smoothing is expected to affect the composition of the accelerated particles (Eichler 1979). Drury, Axford and Summers (1982) show analytically that when k is independent of energy, the smoothing causes the dominant accelerated species (i.e. protons) to have a steeper spectrum than in the case of an infinitely thin shock. Minor species which are only partially stripped could have larger diffusion coefficients than the protons if the diffusion mean free path is rigidity dependent, and therefore for them $k>\bar{k}$. Drury, Axford and

Summers (1982) show that the spectrum of such minor species is flatter than for protons and approaches that of an infinitely thin shock.

Ellison (1981b) has studied these effects with a Monte Carlo calculation appropriate for a parallel shock. In this treatment, the plasma flow and the energetic protons are required to conserve mass, momentum and energy flux, the mean free path is assumed to be proportional to gyroradius, and particles are injected from the shocked plasma downstream in which the temperatures of different ions are proportional to their mass. Ellison (1981b) finds that the shock is indeed broadened and that there are modest enhancements of energetic particles which increase with the mass-to-charge ratio.

The acceleration time in shock acceleration can be obtained from the time-dependent solution of equation (19). Such solutions have been obtained for various initial conditions and geometries by Fisk(1971), Forman and Morfill (1979) and Toptygin (1980) and have been reviewed by Axford (1982). The general result is that

$$\frac{dE}{dt} = \frac{\Delta V}{c} \left(\frac{\lambda_1}{V_1} + \frac{\lambda_2}{V_2}\right)^{-1} \left(E(E+2M\ c^2)\right)^{1/2} \tag{27}$$

This expression shows explicitly that if the mean free path on either side of the shock is very large, the rate of energy gain is very small. Since, as already mentioned, shocked gas downstream is expected to be turbulent, the efficiency of of the acceleration depends critically on the presence of turbulence upstream.

In the absence of upstream turbulence, particles can still be accelerated stochastically by the shock-generated turbulence downstream. By comparing equations (18) and (27) we find that the ratio of the shock acceleration rates and the stochastic acceleration rate downstream is of the order

$V\Delta V/(\delta V)^2\ (\lambda_2/(\lambda_1 + \lambda_2))$, where δV is the velocity of the turbulent elements and λ_2 and λ_1 are the downstream and upstream mean free paths, respectively. Thus, if the mean free paths are comparable, shock acceleration will be more rapid since V and ΔV are expected to be larger than δV.

c. Acceleration in Direct Electric Fields

The previous two sub-sections have dealt with mechanisms that can be best applied to the acceleration of ions in solar flares. In addition to stochastic and shock acceleration, there is also the possibility of accelerating particles in direct electric fields. Such fields are associated with magnetic reconnection in the vicinity of magnetic neutral points and current sheets (Syrovatskii 1981), where they appear perpendicular to the magnetic field. Particle acceleration is also possible in electric fields parallel to the magnetic field (Colgate 1978). Parallel electric fields arise from the interruption (due to plasma instabilities) of the parallel currents associated with twisted magnetic flux tubes and from the formation of double layers of electric charge (e.g. Spicer 1982).

The application of direct electric fields to the acceleration of nonrelativistic electrons in solar flares has been discussed most recently by Spicer (1982). (See also Smith 1979, Heyvaerts 1981). Here we wish to emphasize the role that direct electric fields could play in the very rapid production of ions and the acceleration of relativistic electrons.

As discussed in subsections (a) and (b), both stochastic and shock acceleration could accelerate ions quickly enough to account for the gamma-ray observations, but it is not clear that the mean free paths are, in fact, sufficiently short and the turbulent and shock velocities are large enough to account for the rapid acceleration. On the other hand, in an electric field model (such as that of Colgate 1978), the acceleration time could be as short

as 0.1 sec for a loop of length ~ 10^9cm.

Relativistic electrons around 10 MeV, however, cannot be produced fast enough and in sufficient quantities in stochastic and shock acceleration because the particle energy gain per collision is proportional to particle mass. But there seems to be a good correlation between interplanetary electrons of such energies and gamma-ray flares (Evenson, Meyer and Yanagita 1981; Section IIb). Since the gamma rays are produced by ions of ~ 10 MeV/nucleon, this correlation could indicate electron and ion acceleration to the same energy by an electric field.

In this Section, we review particle acceleration processes in current sheets and in the vicinity of magnetic neutral points. For discussions of acceleration by parallel electric fields, the reader should consult Colgate (1978), Smith (1979), Heyvaerts (1981), and the review of Spicer (1982).

Current sheets and magnetic neutral points are involved in a wide variety of contexts in solar physics. The primary energy release in solar flares may occur by magnetic reconnection (e.g. Kahler et. al. 1980, Sturrock 1980). Parker (1979 and references therein) has emphasized the near-singular conditions required for magnetostatic equilibrium, and has proposed that the reconnection of tangled magnetic fields occurs routinely and inevitably in nature. Syrovatskii (1981) has recently reviewed the formation of current sheets. In view of the important role suggested for current sheets and reconnection in the solar atmosphere it is natural to consider particle acceleration mechanisms associated with these phenomena. Reconnection and associated particle acceleration have been extensively studied in the Earth's magnetosphere (Stern and Ness 1982).

In models of steady state reconnection, magnetic fields of opposite polarity are brought together by a flow of fluid. A detailed discussion of

the fluid theory of steady state reconnection has been given by Vasyliunas (1975). Early descriptions of the reconnection process and its application to solar flares were given by Parker (1957, 1963) and Sweet (1958). Two of the best known examples of reconnection are the models of Petschek (1964) and Sonnerup (1970) which involve x-type neutral points. The magnetic field lines are sketched in Figures 10a and 10b for these two models. These field lines lie in a plane (say, the x-y plane) and there is a constant electric field, **E**, perpendicular to that plane. The electric field is related to the magnetic field B, flow velocity V, and current J in the plasma by Ohm's law

$$E + V \times B/c = \eta J, \qquad (28)$$

where η is the resistivity. The inclusion of other terms in equation (28) is discussed by Vasyliunas (1975). The resistive term is unimportant everywhere except in a small region near the x-type neutral point where **B** becomes small and J is large (because the gradients of B are large). Here the frozen in condition of the magnetic field is violated. Rather than being transported by the fluid, the field diffuses through the semi-stagnant plasma. The region, therefore, is referred to as the diffusion region.

As shown in Figure 10, cold fluid flows inward along the x axis. Most of the fluid never enters the diffusion region, but passes through a shock front (or pair of fronts, in Sonnerup's model) and flows out parallel to the y axis. In Petschek's model, the inflow occurs at a small fraction ($\sim$.1) of the Alfven speed, while the outflow is exactly Alfvenic. This acceleration takes place at the expense of magnetic energy. In Sonnerup's model, the inflow can be faster than in Petschek's model, in which case, less acceleration of the bulk flow occurs. In both models, however, the thermal speed of the ions

increases across the shock front to about the Alfven speed. The increase of electron thermal energy depends on the structure of the shock and the nature of the coupling between electrons and ions.

Similar results have been obtained by Hayashi and Sato (1978) who have simulated time dependent, compressible reconnection by solving the fluid equations numerically. In their model, an initially planar neutral sheet is compressed into an x-type neutral line by imposed fluid flow directed inward, perpendicular to the initial field lines. They assume that when the current density J exceeds some critical value J_c, anomalous resistivity develops and increases as a power of $J - J_c$. Thus, reconnection of the magnetic field-lines and Joule heating of the plasma near the neutral line begin when the neutral sheet has been sufficiently compressed by the incoming flow. They find that, as in the analytic models of reconnection, the regions of inflow and outflow are separated by shocks and that the outflow speed is on the order of the Alfven speed.

If ions gain flow velocities on the order of the Alfven velocity, their energy per nucleon is $2.5 \times 10^4\ B^2/n$, where B is in gauss and n in cm^{-3}. While for most combinations of B and n in the solar atmosphere this energy is not as high as the observed particle energies, this bulk flow acceleration could nonetheless be important as an injection mechanism. In certain exceptional cases, however, B could be high enough and n low enough for the particles to achieve energies as high as 10 MeV/nucleon (e.g. Sonnerup 1973) which would suffice, for example, for the production of nuclear gamma rays.

In addition to the acceleration and heating of the plasma as it passes through the reconnection region, the possibility exists of direct particle acceleration in the electric field at the magnetic null line.

An example of such acceleration was discussed by Speiser (1965). He

considered a magnetic field with field lines parallel to the y axis with field reversal at x = 0,

ORIGINAL PAGE IS
OF POOR QUALITY

$$\mathbf{B} = \mathbf{e_y} B_1 \frac{x}{d}, \quad |x|<d$$
$$\mathbf{B} = \mathbf{e_y} B_1 \frac{x}{|x|}, \quad |x|>d \quad , \tag{29}$$

where $\mathbf{e_y}$ is the unit vector in the y direction and B_1 is a constant. Here the field equals B_1 for $|x|>d$ and goes linearly to zero for $|x|<d$. A constant electric field $\mathbf{E} = VB_1\mathbf{e_z}/c$ is also present and assumed to be continuous at x=0. Everywhere in space except near the field reversal region at x=0, the particle orbits consist of gyration in the x-z plane (the usual Larmor motion) combined with the **ExB** drift in the x direction, toward the plane x=0. Since for $|x|>d$ the motion in z is oscillatory, the average energy gain is zero in this region. However, once a particle has drifted to near the x=0 plane where the field is very weak, it does not gyrate - it is simply accelerated in the z direction. The final energy, E, of the particle depends on the extent, L, of the current sheet in the z direction. Numerically, E in MeV equals 10^{-6} BLV, where B is in gauss, L in km and V km/sec. Thus particles can be accelerated to tens of MeV if B,V and L are large enough.

Whether neutral sheets have sufficient lengths, and, whether or not particles can remain in the sheet for such lengths, are problems which have not yet received clear-cut answers for solar flares.

In order to estimate the distance the particles stay in the neutral sheet, particle orbits in various magnetic geometries have been calculated by Speiser (1965), Friedman (1969), Bulanov and Sasorov (1976), Bulanov (1980), and Syrovatskii (1981). The results depend strongly on assumed geometries,

and analytic treatments can only be made for the simplest field configurations. Time dependent electric and magnetic fields have also been considered (Burke and Layzer 1969, Levine 1974). Levine extended Burke and Layzer's work by trying to estimate the effect of Coulomb collisions between the test particles and field particles in the ambient medium. The existence of an energy loss mechanism which competes with acceleration sets an upper limit on the time constant for collapse of the neutral sheet such that particle acceleration can still occur. Recently, Mullan and Levine (1981) have studied the implications of the collapsing magnetic neutral sheet model for the composition of solar flare accelerated ions (see Section IIb).

Attempts have also been made to calculate the energy spectrum of particles accelerated in neutral sheets. In the absence of stochastic processes such as Coulomb collisions or wave-particle interactions, the phase space distribution function f of the test particles satisfies Liouville's theorem; the density of particles in phase space is constant on phase space trajectories. Therefore, given an initial spatial distribution of injected particles and solutions for the particle orbits, the momentum distribution function of particles leaving the acceleration region can be calculated. (Bulanov and Sasorov 1976, Bulanov 1980). They find that when the initial distribution of particles is uniform in space, the spectrum is an exponential in energy or in a fractional power of the energy. Energy spectra have also been calculated numerically by Bulanov (1980) who finds good agreement with the analytic results. Friedman (1969) has used numerical techniques to calculate final energies for test particles in Petschek's (1964) reconnection model. A generally recognized problem with particle acceleration in neutral sheets is that only very few particles are accelerated.

IV. SOLAR FLARE ENERGY SPECTRA IN INTERPLANETARY SPACE

The spectra of particles observed at any one time in interplanetary space are not exactly the same as the spectra released at the Sun because of velocity dispersion caused by energy-dependent diffusion, and because the solar wind convects and decelerates energetic particles as it expands. If these solar wind effects are small, the effect of velocity dispersion can be eliminated in prompt, magnetically well-connected events by using the time-of-maximum (TOM) energy spectrum formed by the maximum intensity at each energy (Lin 1970, Van Hollebeke et al. 1975). We justify this method below.

At energies less than about 1 MeV/nucleon for ions and 1 keV for electrons, convection and adiabatic deceleration will make the TOM spectrum flatter than the spectrum at the Sun, but the precise effect on the spectrum is uncertain. In addition, the TOM spectrum becomes less reliable for such low-energy particles because their propagation becomes more sensitive to inhomogeneties in the solar wind and magnetic fields (e.g. shocks).

The important questions which need to be resolved before interplanetary spectra can be used to test models of the acceleration and release process at the Sun are: What is the most convenient way to estimate the spectrum at the Sun from spacecraft observations of energetic flare particles; above what energy is that spectrum reliable; and what is the approximate nature of the change in the spectrum below that energy. First, we show why the TOM spectrum in simple well-connected events is a good approximation to the spectrum at the Sun.

The observed $f(p,r,t)$ is related to the spectrum injected into interplanetary space by the transport equation.

$$\frac{\partial f}{\partial t} - \nabla\cdot(k\cdot\nabla f) + V\cdot\nabla f - \frac{\nabla\cdot V}{3}\, p\, \frac{\partial f}{\partial p} = F_0(p,\theta,t)\, \frac{\delta(r-r_0)}{4\pi r^2}\ , \qquad (30)$$

which is analogous to equation (19) for shock acceleration. Here $4\pi p^2 f_0(p,\theta,t)/v$ is the number of particles released per (energy-sec) at momentum p, longitude θ, time t, and radial distance r_0 from the Sun, and **V** is the solar wind velocity.

It is clear that F_0 can be most reliably recovered from f(p,r,t) when F_0 and the interplanetary parameters k and V are as uncomplicated as possible. Therefore, we consider only events in which the effects of delayed and longitude-dependent release at the Sun, longitudinal transport in interplanetary space and all interplanetary propagation complexities (e.g. shocks) are minimal. These are the magnetically well-connected and prompt events at solar longitudes in the range $60^0 \pm 40^0$ west of central meridian. In addition, the spectrum can be derived with confidence only for those events in which the particle fluxes have weak anisotropies during and after the time of maximum (indicating sudden release) and which have smooth time profiles (indicating that the injection is uniform over the connection longitudes). In such simple events, the particle propagation can be treated as spherical diffusion along each field line.

When, furthermore, $k \ll Vr$ and for times $t \ll r/V$, the convection and adiabatic deceleration can be neglected. Then equation (30) reduces to simple time-dependent spherical diffusion from a point source. If the outer boundary is far away, the solution of equation (30) for k independent of r is (Parker 1965)

ORIGINAL PAGE IS
OF POOR QUALITY

$$f(p,r,t) = \frac{N_0(p)}{4\pi p^2} \frac{\exp(-r^2/4tk(p))}{2\sqrt{\pi}\,(tk(p))^{3/2}} \quad , \tag{31}$$

where $N_0(p)dp$ is the number of particles between p and p+dp released at the Sun. Clearly, if the assumptions so far are valid, f(t) will have the time dependence in equation (31), and a fit of particle data to that form will confirm the asumptions and determine $N_0(p)$.

A more direct approach is to note that equation (31) has a maximum at $t_m = r^2/6k(p)$, and that for particles at their $t_m(r,p)$

$$f(p,r,t_m(r,p)) = \frac{(6/e)^{3/2}}{2\sqrt{\pi}r^3} \frac{N_0(p)}{4\pi p^2} = \frac{0.93}{r^3} \frac{N_0(p)}{4\pi p^2} \quad . \tag{32}$$

This is the basis for the assertion that the TOM spectrum is the same as that released at the Sun. If $k \propto r^b$ with b<2, a similar relation holds and $N_0(p)$ $4\pi p^2 f(p,r,t_m)r^3$.

Many of the assumptions leading to the validity of the TOM spectrum break down at low ion energies because of the long time to maximum (~ 1 day at 1 MeV/nucleon) and because of the stronger coupling to the solar wind, which is highly variable on time scales of 1 day. In addition, the condition $Vr \ll k$, which allows convection and adiabatic deceleration to be neglected, is equivalent to $v \gg 3Vr/\lambda$. With $\lambda \sim 0.1$ AU as in Figure 11 (Palmer 1982), this velocity is ~ 10^9 cm/sec, or energies >> 1 MeV/nucleon.

The effect of adiabatic deceleration on the TOM spectrum can be estimated several ways, which give similar results. Scholer (1976) has shown by

numerical simulations of particle trajectories that when $k \lesssim Vr$ and k depends on energy, convection and adiabatic deceleration not only make the time of maximum flux of particles observed at energy E earlier than $r^2/6k(E)$, but make the discrepancy larger at lower energies. This is because particles observed at energy E had higher energy near the Sun and so diffused faster there; the effect increases at lower energies because the relative energy change is larger at lower energies. The energy change must be less than the energy shift in the $t_m(E)$ curve compared to $r^2/6k(E)$. This behavior of t_m is discussed by Kurt et al. (1981) who show that while the t_m vs. energy curves for well-connected flares vary $\propto 1/v$ (as expected for $\lambda \sim$ constant) above an energy E_1 ($\sim$ 1 MeV), the variation is weaker below E_1 in the manner of Scholer's (1976) simulations. The break energy E_1 varies slightly from flare to flare, but is always near where $Vr = k$, on the basis to the t_m at high energies. Kurt et al. (1981) also show that the TOM spectra of these flares are flatter below E_1 than above E_1, and they discuss the apparent energy change, and its effect on the TOM spectrum.

Scholer (1976) found the energy change for each particle by integrating the adiabatic deceleration law $dp/dt = - 2Vp/3r$ along the computed spatial trajectories of the particles. Kurt et al. (1981) approximate the trajectories with diffusion speed $U(p,r)$ such that $dr = Udt$. Then with $U = 3ak/r$, where $k \propto E^a$, the deceleration law can be integrated. It can be shown that $U = 2\ k/r$ is a better choice, consistent with certain analytic results on the effect of convection and adiabatic deceleration on the time of maximum and the particle flux at that time (Fisk and Axford 1968, Forman 1970, The energy change law then becomes $dp/dr = - Vp/3k$. When λ is constant, this results in a change in the speed of a non-relativistic particle, given by $\Delta v = - vr/\lambda$ between the Sun and r. For the typical value of $\lambda = 0.1$ AU, this is

$\Delta v \sim (-\ 4\times10^8\ r(AU))$ cm/sec.

Figure 12 shows the effect of this adiabatic energy change on the spectrum.

We conclude that the TOM spectra of solar flare particle fluxes in interplanetary space is a good first-order estimate of the spectrum released at the Sun, for reasonably well-connected flares showing fairly rapid particle release, down to energies where convection and adiabatic deceleration are significant. The TOM spectrum should be used because it eliminates the velocity dispersion caused by the energy-dependence of the diffusion coefficient; the spectrum varies slowly at that time; it is relatively insensitive to finite injection times; and it is early enough that convection and adiabatic deceleration effects are minimal. The TOM spectrum begins to deviate from the spectrum injected at the Sun at energies where $k(E) \lesssim Vr$; that is $E < E_1 \sim 3(r/10\lambda)^2$ MeV/nucleon for ions and $\lesssim 1.5\ (r/10\lambda)^2$ keV for electrons, or when the time of maximum is longer than the solar wind transit time divided by the Compton-Getting factor. Typical values of λ make $E_1 \sim 1$ MeV/nucleon for ions and ~ 1 keV for electrons.

The effect of adiabatic deceleration and convection on ion spectra with realistic propagation parameters below a few MeV/nucleon is not known exactly. We have presented some rules which describe approximately how the TOM spectrum is related to the spectrum released at the Sun. Since, as we have shown in Section III, the spectrum below 1 MeV/nucleon differs greatly between acceleration theories which explain the spectrum above 1 MeV/nucleon equally well, a more exact method of deducing the accelerated spectrum below 1 MeV/nucleon from that observed in interplanetary space is needed to decide among such theories. However, because the propagation of such low-energy ions is extremely sensitive to interplanetary conditions, it is problematic whether

this can be practically done with observations at 1 AU.

V. SUMMARY AND OUTLOOK

We have reviewed observations and theories of particle acceleration in solar flares. Flare accelerated particles that remain trapped at the Sun produce a variety of electromagnetic emissions which provide important information on the timing of the acceleration and on the number and energy of the accelerated particles. While it is clear that not all particles species are accelerated to their final energies at the same time, the distinction between first-phase and second-phase acceleration is no longer as clear as it had been prior to recent gamma-ray observations. There is ample evidence for the bulk energization of non-relativistic electrons whose interactions in the solar atmosphere produce hard X rays. The energy contained in these electrons constitutes a major fraction of all the available flare energy. The acceleration of the gamma-ray producing ions in some flares is closely associated in time with this bulk energization. The energy content of these ions, while smaller than that of the non-relativistic electrons, also constitutes a significant fraction of the total flare energy (Section IIa).

The ions observed in interplanetary space are probably accelerated by shocks or turbulence. The correlation between Type II radio bursts and ions events provides the main observational support for this conclusion. Both stochastic and diffusive shock acceleration can explain the observed energy spectra, but the fact that these spectra do not vary much from one event to another (Section IIb) seems to imply that one of these mechanisms is dominant. The relative importance of stochastic and shock acceleration depends on the injection thresholds, the relative magnitudes of the shock and

turbulent speeds and on the magnitudes of the scattering mean free paths. The existence of suitable turbulence ahead of the shock is an essential requirement for shock acceleration (Section IIIb).

The chemical compositions of the energetic particles in space and their variability appears to be a problem of injection (Section IIb). This follows from the fact that abundance variations are generally not accompanied by spectral variations. Both stochastic and shock acceleration mechanisms have injection thresholds, but the threshold of shock acceleration is expected to be higher than that of stochastic acceleration (Section III). The abundance variations could be due to variations of the threshold energies, or of the preheating conditions. Preheating or preacceleration are required to produce particles above the thresholds.

Both stochastic and shock acceleration can be rapid enough to produce the observed rise times of the gamma-ray emission. We find that the necessary short scattering mean free paths are not inconsistent with other data.

The question of whether the ions responsible for gamma-ray production and those observed in interplanetary space are produced by the same mechanism remains unanswered. On the one hand, the energy spectra of these two populations appear to be similar, but on the other, the correlation between the number of particles seen in space and inferred at the Sun is quite poor. An important recent observation (Section IIa) has been that of relativistic electrons seen in interplanetary space in correlation with gamma-ray emissions. Since stochastic and shock acceleration are not expected to accelerate relativistic electron efficiently, this might be an indication for the acceleration of nuclei and electrons to essentially the same energies in electric fields (Section IIIc).

Both observational and theoretical work is required for future progress

in the understanding of solar flare particle acceleration. On the observational side, much progress has recently been achieved by such novel investigations as gamma-ray and neutron observations, X-ray observations with high temporal resolution, and direct charged particle detections with good spectral elemental, isotopic and ionic resolutions. These should be continued and correlated with each other as well as with other data on solar flares such as shock parameters. For example, in energetic particle measurements there is a need for greater sensitivity. Some of the most bizarre and interesting flare events are the small ones; however, existing instrumentation cannot accumulate sufficient statistics to measure the composition in great detail. More sensitive gamma-ray observations are needed in order to determine whether prompt ion acceleration is present in all flares. Gamma-ray observations with high energy resolution are also needed to resolve the lines and measure Doppler shifts which would provide information on energetic particle beaming.

The theoretical and interpretative work making use of the existing observations is just beginning. We can foresee important advances from studies that will apply recent theoretical results on shock acceleration to solar flare acceleration, investigations of ion acceleration by electric fields leading to the beaming of the energetic particles which could have observable effects on gamma-ray spectra, and from a much more detailed study of acceleration theories which would consider the acceleration of particles and their effect on the accelerating agent in a self consistent manner.

Acknowledgments

We wish to acknowledge W. I. Axford, G. A. Dulk, P. Evenson, D. C. Ellison, D. J. Forrest, M. L. Goldstein, J. R. Jokipii, R. P. Lin, R. E. McGuire, D. F. Smith and M. A. I. Van Hollebeke for useful discussions, and D. V. Reames for providing the use of unpublished data. The research described in this paper was supported by NASA's Solar Terrestrial Theory Program. E. G. Z. wishes to thank the Aspen Center for Physics where part of her research was carried out.

TABLE 1

Flare	W_d(>1 MeV/n)	W_{esc}(>1 MeV/n)	W_e(>20 keV)	$\bar{N}_p$(>10 MeV)	$N_{esc,p}$(>10MeV)
Aug 4, 1980	2.5×10^{30}erg	3×10^{31}erg	2×10^{32}erg	1.3×10^{34}	3×10^{35}
June 7, 1972	2×10^{29}erg	2×10^{27}erg	4×10^{30}erg	8.5×10^{32}	10^{31}

REFERENCES

Abramowitz, M. and Stegun, I. A.: 1965, Handbook of Mathematical Functions, New York: Dover Publications.

Achterberg, A. and Norman, C. A.: 1980, Astron. and Astrophys. 89, 353.

Achterberg, A.: 1981, Astron. and Astrophys. 97, 259.

Anglin, J. D., Dietrich, W. F., and Simpson, J. A.: 1977, 15th Internat. Cosmic Ray Conf. Papers, Plovdiv, 5, 43.

Asbridge, J. R., Bame, S. J., and Strong, I. B.: 1968, J. Geophys. Res., 73, 5777.

Axford, W. I., Leer, E. and Skadron, G.: 1977, Proc. 15th Int'l Cosmic Ray Conf., Plovdiv, 11, 132.

Axford, W. I.: 1982, in (ed.) Tuyenne, T. D. and Levy, T., Plasma Astrophysics, ESA publication SP-151.

Bai, T.: 1982, in R. E. Lingenfelter, H. S. Hudson and D. M. Worrall (eds.), Gamma-Ray Transients and Related Astrophysical Phenomena, New York: Inst. of Phys., p. 409.

Bai, T. and Ramaty, R.: 1976, Solar Phys. 49, 343.

Bai, T. and Ramaty, R.: 1979, Astrophys. J., 227, 1072.

Barbosa, D. D.: 1979, Astrophys. J. 233, 383.

Barnes, G. W. and Simpson, J. A.: 1976, Astrophys. J., 210, L91.

Bertsch, D. L., Fichtel, C. E. and Reames, D.V.: 1969, Astrophys. J. Lett., 157, L53.

Blandford, R. P. and Ostriker, J. P.: 1980, Astrophys. J. 237, 793.

Brown, J. C.: 1971, Solar Phys. 18, 489.

Brown, J. C. and Smith, D. F.: 1980, Reports on Progress in Physics, 43, 125.

Bryant, D. A., Cline, T. C., Desai. U. D. and McDonald, F. B.: 1965, Astrophys. J. 141, 478.

Bulanov, S.V.: 1980, Sov. Astron. Lett., 6, 206.

Bulanov, S.V. and Sasorov, P. V.: 1976, Sov. Astron. 19, 464.

Burke, J. R., and Layzer, D.: 1969, Astrophys. J., 157, 1169.

Canfield, R. C. and Cook, J. W.: 1978, Astrophys. J. 225, 650.

Chen, G. and Armstrong, T. P.: 1975, Proc. 14th Int'l Cosmic Ray Conf. (Munich) 5, 1814.

Chubb, T. A.: 1970 in E. R. Dryer (ed.), Solar-Terrestrial Physics (Proc. Int. Symp. on Solar-Terrestrial Physics, Leningrad (1970), Part 1, p. 99.

Chupp, E. L.: 1982, in R. E. Lingenfelter, H. S. Hudson and D. M. Worrall (eds.), Gamma-Ray Transients and Related Astrophysical Phenomena, New York: Amer. Inst. of Physics, p. 363.

Chupp, E. L. et al.: 1973, Nature, 241, 333.

Chupp, E. L. et al.: 1982, Astrophys. J. Letters (in press).

Colgate, S. A.: 1978, Astrophys. J., 221, 1068.

Colgate, S. A., Audouze, J. and Fowler, W. A.: 1977, Astrophys. J. 213, 849.

Cook, W. R., Stone, E. C., and Vogt, R. E.: 1980, Astrophys. J. Letters, 238, L97.

Crannell, C. J., Frost, K. J., Matzler, C., Ohki, K. and Saba, J. L.: 1978, Astrophys. J. 223, 670.

Datlowe, D.: 1971, Solar Phys. 17, 436.

Datlowe, D. W. and Lin, R. P.: 1973, Solar Phys. 32, 459.

Decker, R. B., Pesses, M. E., and Armstrong, T. P.: 1981, Proc. 17th Int'l Cosmic Ray Conf. (Paris) 3, 406.

Dietrich, W. F.: 1981, Astrophys. J. Letters, 245, L41.

Dietrich, W. F. and Simpson, J. A: 1979, Astrophys. J. Letters, 231, L91.

Dietrich, W. F. and Simpson, J. A.: 1981, Astrophys. J. Letters, 245, L41.

Drury, L. O'C., Axford, W. I., and Summers, D.: 1982, M.N.R.A.S. 198, 833.

Drury, L. O'C. and Volk, H. J: 1981: Astrophys. J., 248, 344.

Duggal, S. P.: 1979, Reviews of Geophys. Space Phys. 17, 1021.

Dulk, G. A., Melrose, D. B. and Smerd, S. F.: 1978, Proc. Astron. Soc. Australia 3, 243.

Eichler, D.: 1979, Astrophys. J. 229, 419.

Eichler, D.: 1981, Astrophys. J. 244, 711.

Ellison, D. C.: 1981a, Geophys. Res. Lett., 8, 991.

Ellison, D. C: 1981b, Monte Carlo Simulation of Collisionless Shock Acceleration, Ph.D. Thesis, Catholic University of America, Washington, D. C.

Evenson, P., Meyer, P. and Yanagita, S.: 1981, Internat. Cosmic Ray Conference Papers, Paris, 3, 32.

Fan, C. Y., Gloeckler, G. and Hovestadt, D.: 1975, in S. Kane (ed.) Solar Gamma, X and EUV Radiations, IAU Symp. 68, p. 411.

Fermi, E.: 1949, Phys. Rev. 75, 1169.

Fichtel, C. E. and Guss, D. E.: 1961, Phys. Rev. Letters, 6, 495.

Fisk, L. A.: 1971, J. Geophys. Res. 76, 1662.

Fisk, L. A.: 1978, Astrophys. J. 224, 1048.

Fisk, L. A. and Axford, W. I.: 1968, J. Geophys. Res., 73, 4396.

Fisk, L. A., and Lee, M. A., 1980, Astrophys. J., 237, 620.

Forman, M. A.: 1971, J. Geophys. Res. 76, 759.

Forman, M. A.: 1981a, Advances in Space Res. 1, 41.

Forman, M. S.: 1981b, Proc. 17th Int'l Cosmic Ray Conf. (Paris) 3, 467.

Forman, M. A., and Morfill, G.: 1979, Proc. 16th Int'l Cosmic Ray Conf., (Kyoto) 5, 328.

Friedman, M.: 1969, Phys. Rev., 182, 1408.

Frost, K. J. and Dennis, B. R.: 1971, Astrophys. J. 165, 655.

Garrard, T. L. Stone, E. C. and Voqt, R. E.: 1973 in R. Ramaty and R. G. Stone (eds.), High Energy Phenomena on the Sun, NASA SP-342, p. 341.

Geiss, J.: 1973, 13th Internat. Cosmic Ray Conf., Denver, 5, 3375.

Gloeckler, G.: 1979, Reviews of Geophysics and Space Physics, 17, 569.

Gloeckler, G., Sciambi, R. K., Fan, C. Y., and Hovestadt, D.: 1976, Astrophys. J. Letters, 209, L93.

Hasselmann, K., and Wibberenz, G.: 1968, J. Geophys., 34, 353.

Hayaski, T. and Sato, T.: 1978, J. Geophys. Res., 83, 217.

Heyvaerts, J.: 1981, in E. R. Priest (ed.) Solar Flare Magnetohydrodynamics, New York, Gordon and Breach, p. 429.

Holman, G. D., Ionson, J. A., and Scott, J.S.: 1979, Astrophys. J., 228, 576.

Hovestadt, D. et al.: 1981, Astrophys. J. Letters, 246, L81.

Hoyng, P., Brown, J. C. and Van Beek, H. F.: 1976, Solar Physics, 48, 197.

Hudson, H. S.: 1972, Solar Phys. 24, 414.

Hudson, H. S.: 1979, in J. Arons, C. McKee and C. Max (eds.), Particle Acceleration Mechanisms in Astrophysics, New York: Amer. Inst. of Phys., p. 115.

Hudson, H. S., Lin, R. P. and Stewart, R. T., 1982, Solar Physics, 75, 245.

Ibragimov, I. A. and Kocharov, G. E.: 1977, Sov. Astron. Letters, 3 (5), 221.

Jokipii, J. R.: 1971, Review of Geophysics Space Physics, 9, 27.

Kane, S. R.: 1980, in P. A. Sturrock (ed.) Solar Flares, Boulder Colorado: Colorado Associated Univ. Press, p. 187.

Kahler, S., Spicer, D., Uchida, Y., and Zirin, H. 1980, in P. A. Sturrock (ed.) Solar Flares, Boulder Colorado: Colorado Associated University Press, p. 83.

Kane, S. R.: 1980, in P. A. Sturrock (ed.) Solar Flares, Boulder Colorado: Colorado Associated Univ. Press, p. 187.

Kleckler, B., Hovestadt, D., Scholer, M., Gloeckler, G., and Ipavich, F. M.: 1982, Trans. Amer. Geophys. Union, 63, 399.

Kocharov, G. E. and Kocharov, L. G.: 1978, Proc. 10th Leningrad Symp. on Cosmic Physics, A. F. Yoffe Physico-Technical Inst., Leningrad, p. 38.

Kozlovsky, B. and Ramaty, R.: 1977, Astrophys. Letters, 19, 19.

Kulsrud, R.M. and Ferrari, A.: 1971, Astrophys. and Space Sci. 12, 302.

Kurt, V. G., Logachev, Ju. I., Stoïpovsky, V. G., and Daiborg, E. I.: 1981, Proc. 17th Int'l Cosmic Ray Conf. 3, 69.

Lee, M. A.: 1982, J. Geophys. Res., ~~(in press)~~.

Lee, M. A. and Fisk, L. A.: 1981, Proc. 17th Int'l Cosmic Ray Conf. (Paris) 3, 405 (and late papers).

Lee, M. A. and Fisk, L. A.: 1982, Space Science Revs. (in press).

Lin, R. P.: 1971, Solar Phys. 15, 453.

Lin, R. P.: 1974, Space Sci. Rev. 16, 189.

Lin, R. P., Meng, C. I. and Anderson, K. A.: 1974, J. Geophys. Res. 79, 489.

Lin, R. P. and Hudson, H. S.: 1976, Solar Phys. 50, 153.

Lin, R. P., Mewaldt, R. A., and Van Hollebeke, M. A. I.: 1982, Astrophys. J. 253, 949.

Lingenfelter, R. E. and Ramaty, R.: 1967, in B.S.P. Shen (ed.) High Energy Nuclear Reactions in Astrophysics, W. P. Benjamin, New York, p. 99.

Levine, R. H.: 1974, Astrophys. J. 190, 447.

Luhmann, J. G.,: 1976, J. Geophys. Res., 81, 2089.

Mason, G. M., Fisk, L. A., Hovestadt, D., and Gloeckler, G.: 1980, Astrophys. J., 239, 1070.

Ma Sung, L. S., Gloeckler, G., Fan, C. Y. and Hovestadt, D.: 1981, Astrophys.

J. Letters, 245, L45.

McDonald, F. B.: 1981, Proc. 17th Int'l Cosmic Ray Conf. (Paris) (rapporteur paper).

McDonald, F. B., Fichtel, C. E. and Fisk, L. A.: 1974, in F. B. McDonald and C. E. Fichtel (eds.), High Energy Particles and Quanta in Astrophysics, Cambridge, Mass: MIT press, p. 212.

McDonald, F. B., Teegarden, B. J., Trainor, J. H., Von Rosenvinge, T. T. and Webber, W. R.: 1976, Astrophys. J. Letters, 203, L149.

McGuire, R. E., Von Rosenvinge, T. T., and McDonald, F. B.: 1979, 16th Internat. Cosmic Ray Conf. Papers, Kyoto, 5, 61.

McGuire, R. E., Von Rosenvinge, T. T., and McDonald, F. B.: 1981, 17th Internat. Cosmic Ray Conference Papers, Paris 3, p. 65.

Melrose, D. B.: 1974, Solar Phys., 37, 353.

Melrose, D. B.: 1980, Plasma Astrophysics, New York: Gordon and Breach.

Mewaldt, R. A., Spalding, J. D., Stone, E. C. and Vogt, R. E.: 1979, Astrophys. J. Letters, 231, L97.

Mewaldt, R. A., Spalding, J. D., Stone, E. C. and Vogt, R. E.: 1981, Astrophys. J. Letters, 243, L163.

Meyer, J. P.: 1981, 17th. Internat. Cosmic Ray Conf. Papers, Paris, 3, p. 145. 149.

Mogro-Campero, A. and Simpson, J. A.: Astrophys. J. Letters, 171, L5.

Mullan, D. J.: 1980, Astrophys. J. 237, 244.

Mullan, D. J. and Levine, R. H.: 1981, Astrophys. J. Suppl., 47, 87.

Ogilvie, K. W., Scudder, J. D., and Olbert, S.: 1978, J. Geophys. Res. 83, 3776.

Palmer, I.A.: Reviews Geophysics Space Physics, 20, 335.

Parker, E. N.: 1957, J. Geophys. Res. 62, 509.

ORIGINAL PAGE IS
OF POOR QUALITY

Parker, E.N.: 1979, Cosmical Magnetic Fields, Oxford: Clarendon Press.

Parker, E. N.: 1963, Interplanetary Dynamical Processes, Wiley, New York.

Parker, E. N. and Tidman, D. A.: 1958, Phys. Rev., 111, 1206.

Pesses, M. E., Decker, R. B., and Armstrong, T. P.: 1982, Space Science Revs. (in press).

Petschek, H. E.: 1964, in W. N. Hess (ed.) Physics of Solar Flares, NASA SP-50 p. 425.

Podosek, F. A.: 1978, Ann. Rev. Astr. Ap., 16, 293.

Price, P. B., Hutcheon, I., Cowsik, R., and Barber, D. J.: 1971, Phys. Rev. Letters, 26, 916.

Prince, T., Ling, J. C., Mahoney, W. A., Riegler, G. R. and Jacobson, A. S.: 1982, Astrophs. J. Letters, 255, L81.

Ramaty, R.: 1969, Astrophys. J. 158, 753.

Ramaty, R.: 1979, in J. Arons, C. McKee and C. Max (eds.), Particle Acceleration Mechanisms in Astrophysics, New York: Amer. Inst. Phys., p. 135.

Ramaty, R.: 1982, in this volume.

Ramaty, R. et. al.: 1980, in P. A. Sturrock (ed.), Solar Flares, Boulder Colorado: Colorado Associated Univ. Press., p. 117.

Ramaty, R. and Crannell, R. C.: 1976, Astrophys. J. 203, 766.

Ramaty, R. and Kozlovsky, B.: 1974, Astrophys. J. 193, 729.

Ramaty, R., Kozlovsky, B., and Lingenfelter, R. E.: 1975, Space Sci. Rev. 18, 341.

Ramaty, R., Kozlovsky, B., and Lingenfelter, R. E.: 1979, Astrophys. J. Suppl. 40, 487.

Ramaty, R., Kozlovsky, B. and Suri, A. N.: 1977, Astrophys. J. 214, 617.

Reames, D. V. and Von Rosenvinge, T. T.: 1981, 17th Internat. Cosmic Ray Conf.

ORIGINAL PAGE IS
OF POOR QUALITY

Papers, Paris, 3, 162.

Richter, A. K. and Keppler, E.: 1977, J. Geophys. Res. 42, 645.

Rienhard, R. and Wibberenz, G.: 1974, Solar Phys. 36, 473.

Rothwell, P. L.: 1976, J. Geophys. Res. 81, 709.

Scholer, M.: 1976, Astrophys. J. 209, L101.

Scholer, M., Ipavich, F. M., Gloeckler, G., Hovestadt, D. and Klecker, B.: 1980, Geophys. Res. Lett. 7, 73.

Sciambi, R. K., Gloeckler, G., Fan, C. Y. and Hovestadt, D.: 1977, Astrophys. J. 214, 316.

Scudder, J. D., Ogilvie, K. W.: 1979, J. Geophys. Res. 84, 6603.

Shea, M. A. and Smart, D. F.: 1973, 13th Internat. Cosmic Ray Conf. Papers, Denver, 2, 1548.

Simnett, G. M.: 1971, Solar Phys. 20, 448.

Skilling, J. A.: 1975, Monthly Not. Ray. Astron. Soc., 172, 557.

Smith, D. F.: 1979, in J. Arons, C. McKee and C. Max (eds.), Particle Acceleration Mechanisms in Astrophysics, New York: Amer. Inst. Phys., p. 155.

Smith, D. F. and Auer, L. H.: 1980, Astrophys. J. 238, 1126.

Smith, D. F. and Goldman, M. V.: 1982, this volume.

Sonnerup, B. U. O.: 1970, J. Plasma Physics 4, 161.

Sonnerup, B. U. O.: 1971, J. Geophys. Res. 76, 8211.

Sonnerup, B. V. O.: 1973, in R. Ramaty, and F. E. Stone (eds.) High Energy Phenomena on the Sun, NASA SP-342, 357.

Speiser, T. W.: 1965, J. Geophys. Res., 70, 4219.

Stern, D. P., and Ness, N. F.: 1982, Ann. Rev. of Astron. and Astrophys. 20 (in press).

Sturrock, P. A.: 1980, in P. A. Sturrock, (ed) Solar Flares, Colo. Assoc.

ORIGINAL PAGE IS
OF POOR QUALITY

Univ. Press,s Boulder, 411.

Suri, A. N., Chupp, E. L., Forrest, D. J. and Reppin, C.: 1975, Solar Phys. 43, 414.

Svestka, Z. and Fritzova, L.: 1974, Solar Phys. 36, 417.

Sweet, P. A.: 1958, NOVO Cimento, Suppl., 8, 188.

Syrovatskii, S. I.: 1981, Annual Revs. Astron. Astrophys., 19, 163.

Takakura, T.: 1960, Publ. Astron. Soc. Japan 12, 325.

Teegarden, B. J., Von Rosenvinge, T. T. and McDonald, F. B.: 1973, Astrophys. J. 180, 571.

Toptygin, I. N.: 1980, Space Sci. Revs. 26, 157.

Tsurutani, B. T. and Rodriquez, P.: 1981, J. Geophys. Res. 86, 4319.

Uchida, Y.: 1974, Solar Phys. 39, 431.

Van Hollebecke, M. A. I.: 1979, Reviews of Geophys. Space Phys. 17, 545.

Van Hollebecke, M. A. I., MaSung, L. S., and McDonald, F. B.: 1975, Solar Phys. 41, 189.

Vasyliunas, V. M.: 1975, Reviews Geophysics and Space Physics 13, 308.

Von Rosenvinge, T. T., Ramaty, R., and Reames, D. V: 1981, 17th Internat. Cosmi Ray Conf. Papers, Paris, 3, p. 28.

Wentzel, D. G.: 1965, J. Geophys. Res. 70, 2716.

Wentzel, D. G.: 1969, Astrophys. J., 157, 545.

Wild, J. P., Smerd, S. F. and Weiss, A. A.: 1963, Ann. Rev. Astron. Astrophys., 1, 291.

Zweibel, E. G. and Haber, D.: 1982, Astrophys. J. (in press).

Zwickl, R. D., Krimigis, S. M., Carbary, J. F., Leath, E. P., Armstrong, T. P., Hamilton, D. C., and Gloeckler, G.: 1981, J. Geophys. Res. 86, 8125.

FIGURE CAPTIONS

Fig. 1. Time dependences of X-rays, gamma-rays and microwave radiation from the 4 August 1972 flare (from Bai and Ramaty 1976).

Fig. 2. Bessel function (see Section IIIa) in velocity,and exponential in rigidity fits to proton and alpha particle spectra for the 5 November 1974 flare particle event. Fit parameters are αT (proton) = 0.024, αT (alpha) = 0.015, R_0 (proton) = 73 MV, R_0 (alpha) = 80 MV.

Fig. 3. Electron energy spectrum from the 7 September 1973 flare (from Lin, Mewaldt and Van Hollebeke 1982).

Fig. 4. Correlation between solar flare electron and proton intensities observed in interplanetary space (from Ramaty et al. 1980).

Fig. 5. Compositon of solar energetic particles relative to the photosphere (see Section IIb for details).

Fig. 6. Energy loss rates of protons, Fe nuclei and electrons in neutral H (dashed curves) and energy gain rates from equation (18) (from Ramaty 1979).

Fig. 7. Energy loss rates of protons and electrons in an H plasma of 2×10^6K (dashed curves). The loss rates for other ions scale as Z^2/A. The energy gain rates are from equation (18) (from Ramaty 1979).

Fig. 8. Time dependent proton and electron spectra from stochastic

acceleration with impulsive injection and no losses, E_0 is the injection energy (from Ramaty 1979).

Fig. 9. Comparison of the particle spectra produced by steady-state stochastic acceleration, equation (13), with shock acceleration, equation (24), for models in which the scattering mean free path, λ, and the escape time, T, are energy independent. V_{sh} is the shock speed and $(\delta V)^2$ the mean square turbulent velocity.

Fig. 10. Magnetic field and flow configuration in (a) the Petchek (1964) and (b) the Sonnerup (1970) reconnection models.

Fig. 11. Mean free paths of solar electrons and protons in interplanetary space deduced by fitting time profiles in many events (from Palmer 1982).

Fig. 12. Illustration of the probable effect of adiabatic deceleration on the spectra of solar flare ions at the time of maximum. The spectrum at the Sun (shown as a dashed line) is shifted to lower energies.

ORIGINAL PAGE IS
OF POOR QUALITY

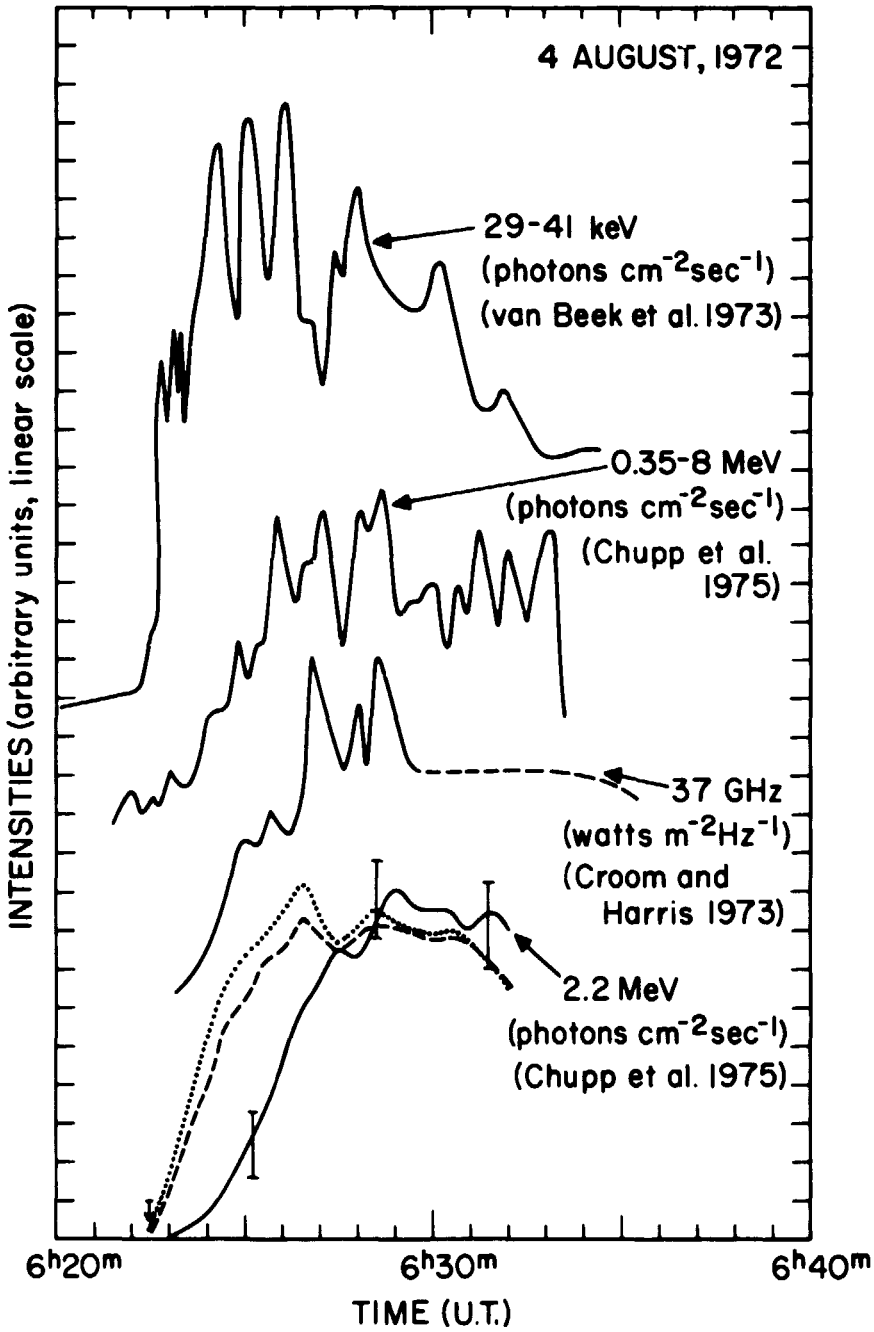

Figure 1

ORIGINAL PAGE IS
OF POOR QUALITY

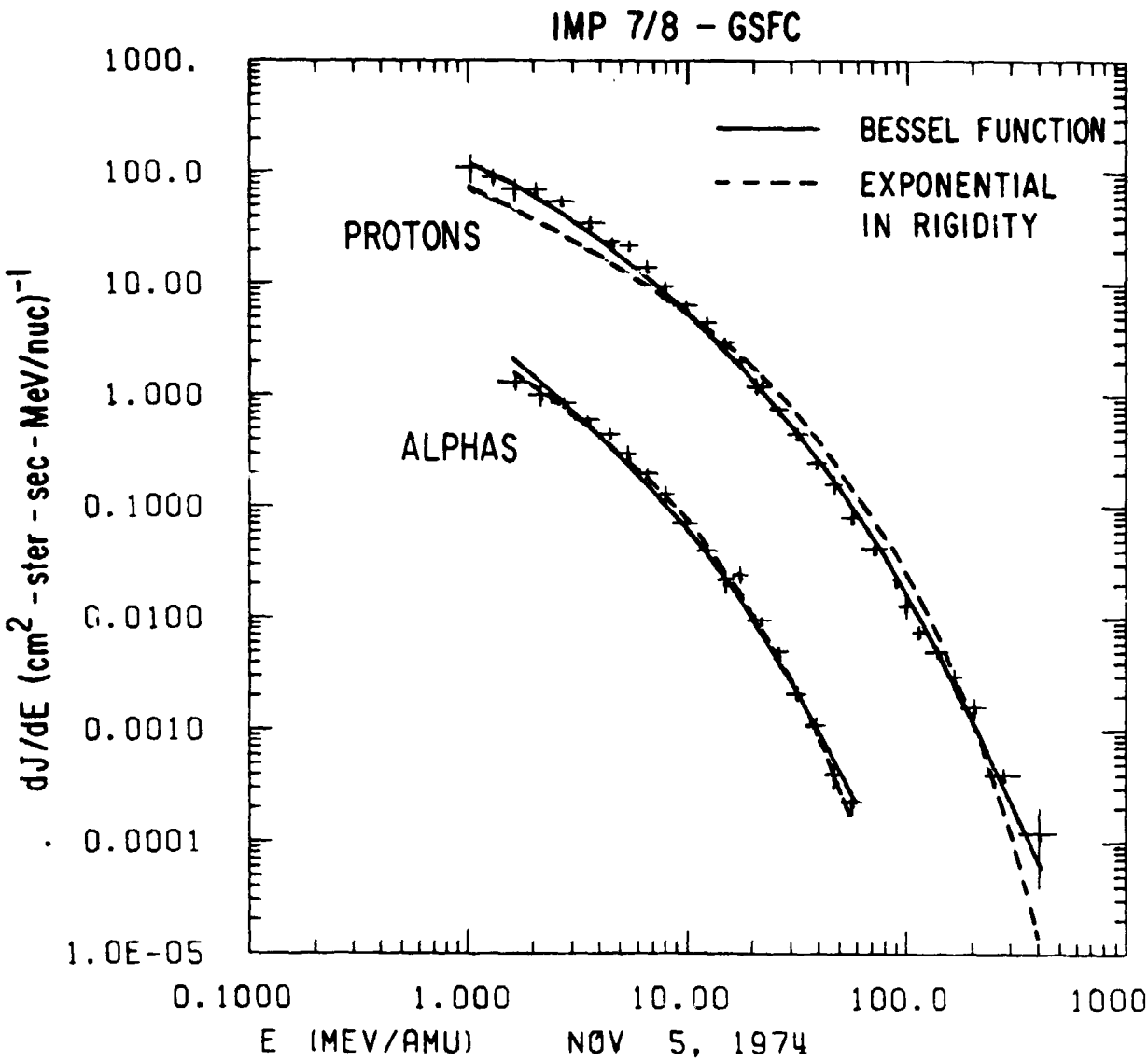

Figure 2

ORIGINAL PAGE IS
OF POOR QUALITY

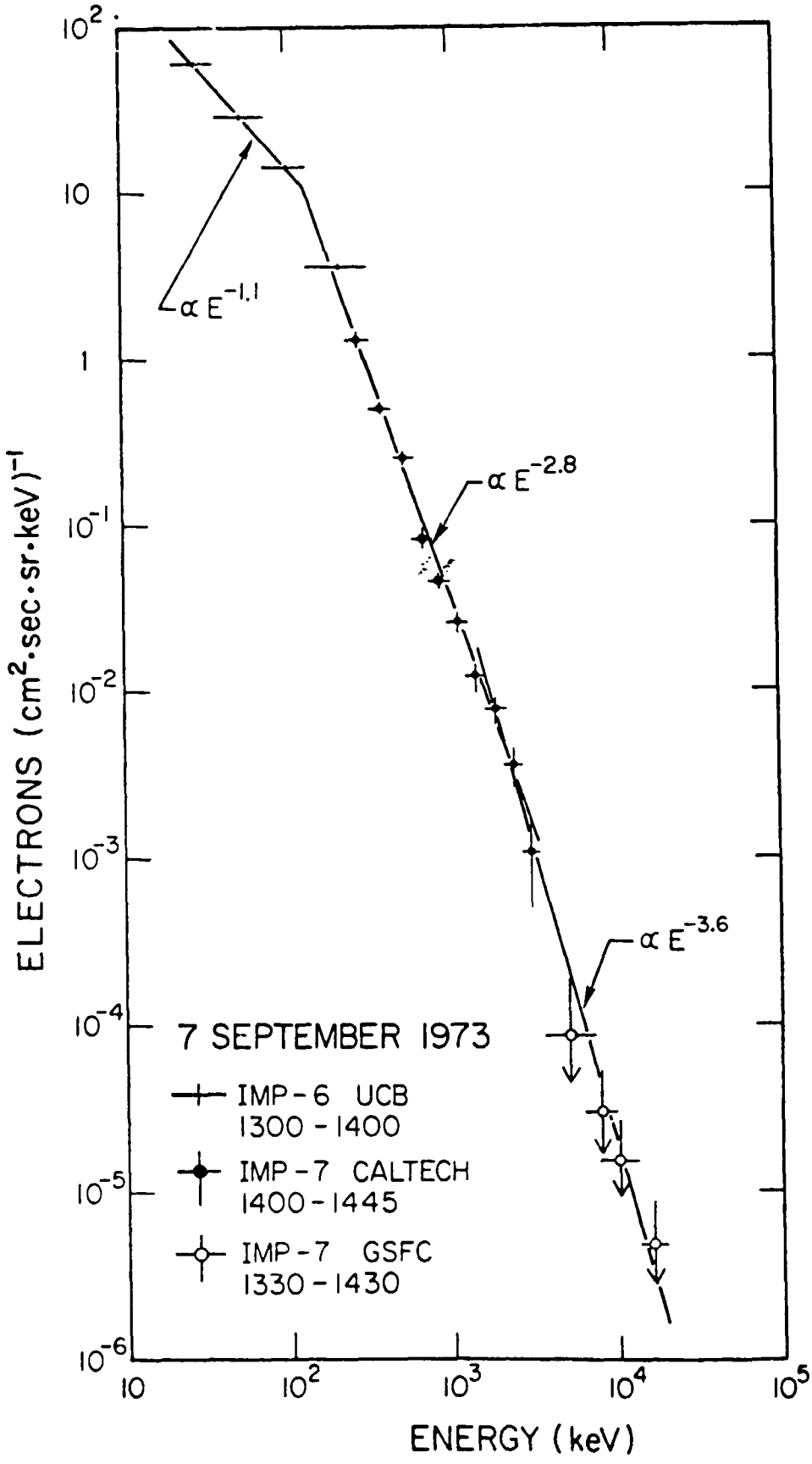

Figure 3

ORIGINAL PAGE IS
OF POOR QUALITY

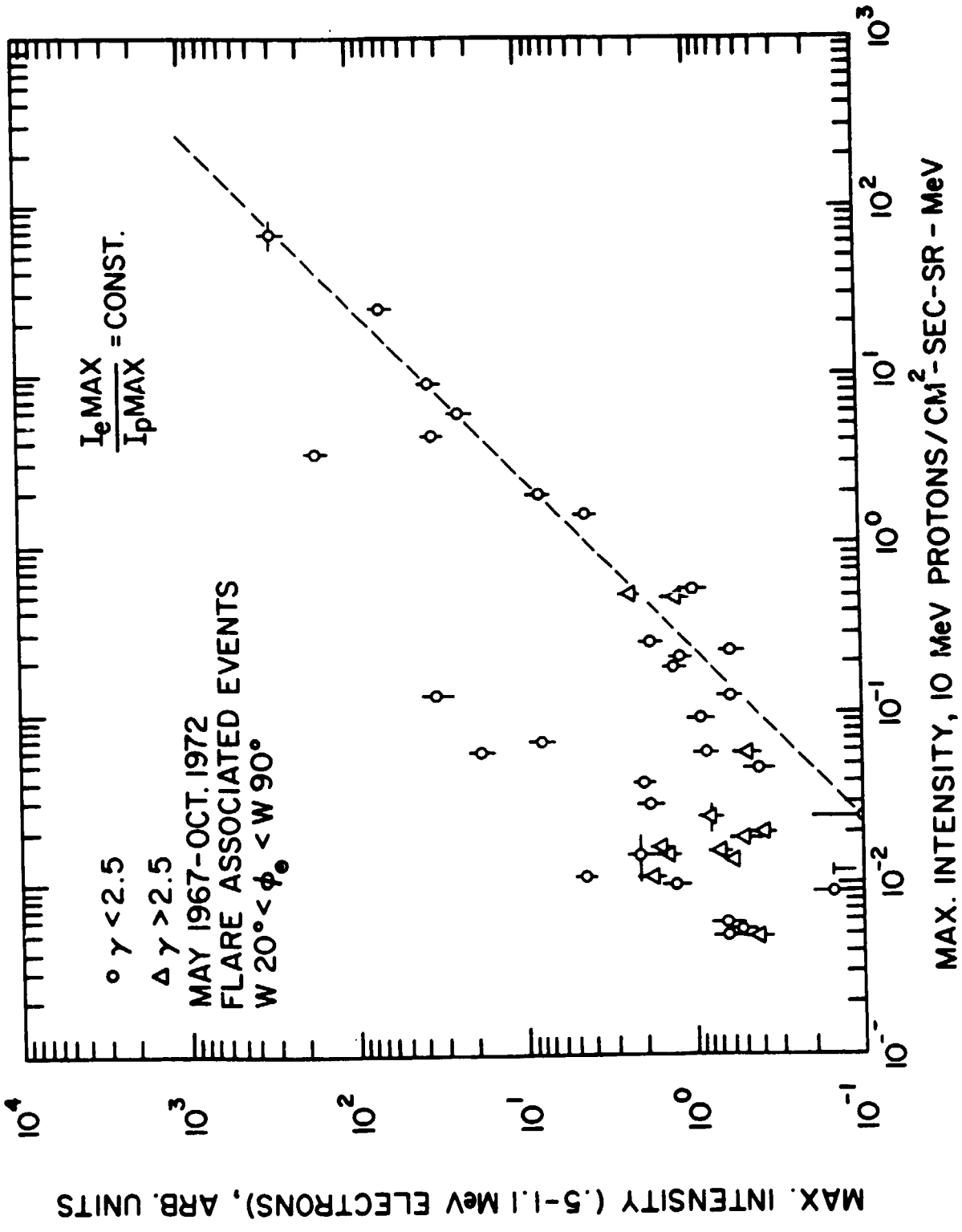

Figure 4

ORIGINAL PAGE IS
OF POOR QUALITY

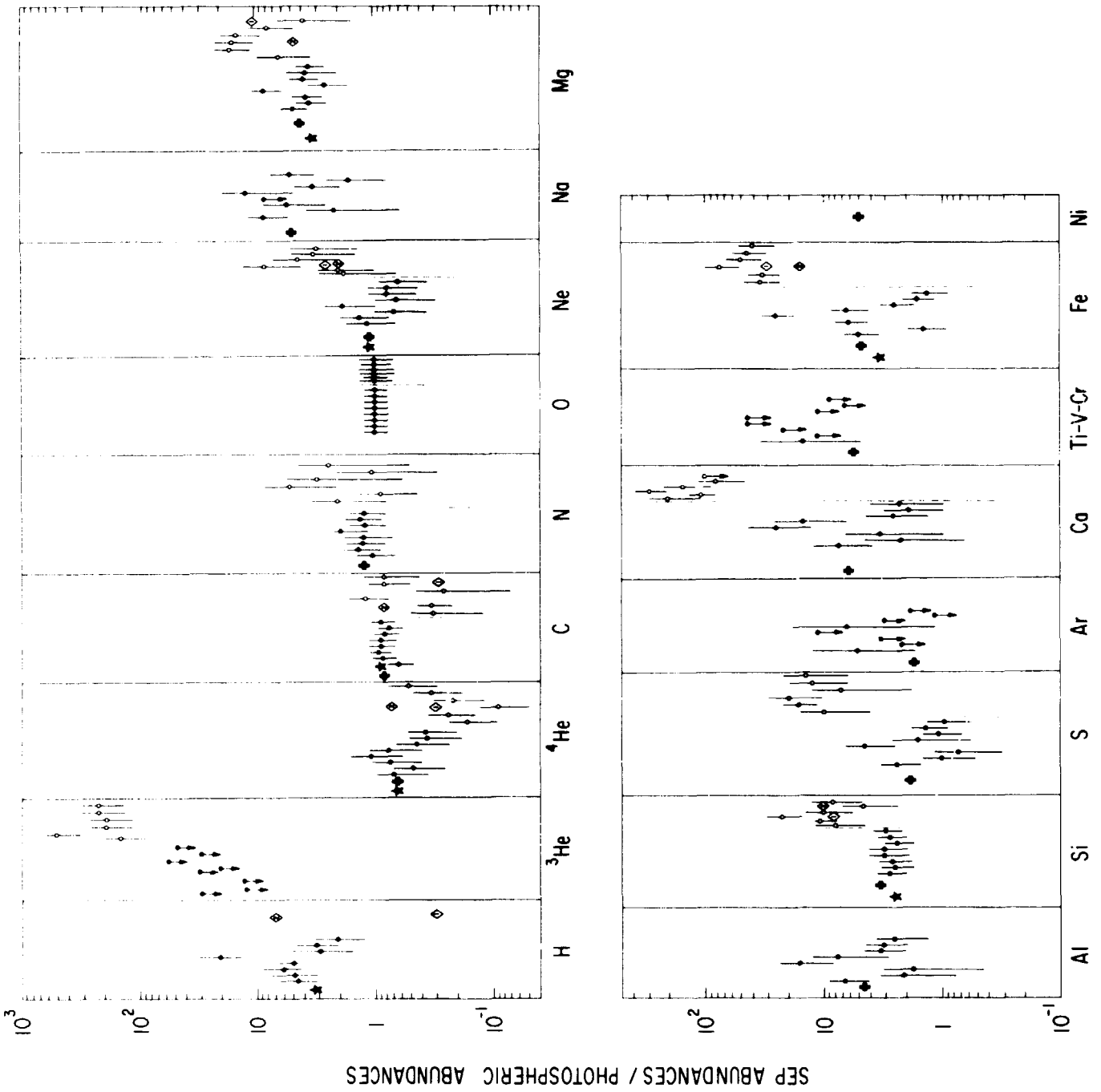

Figure 5

ORIGINAL PAGE IS
OF POOR QUALITY

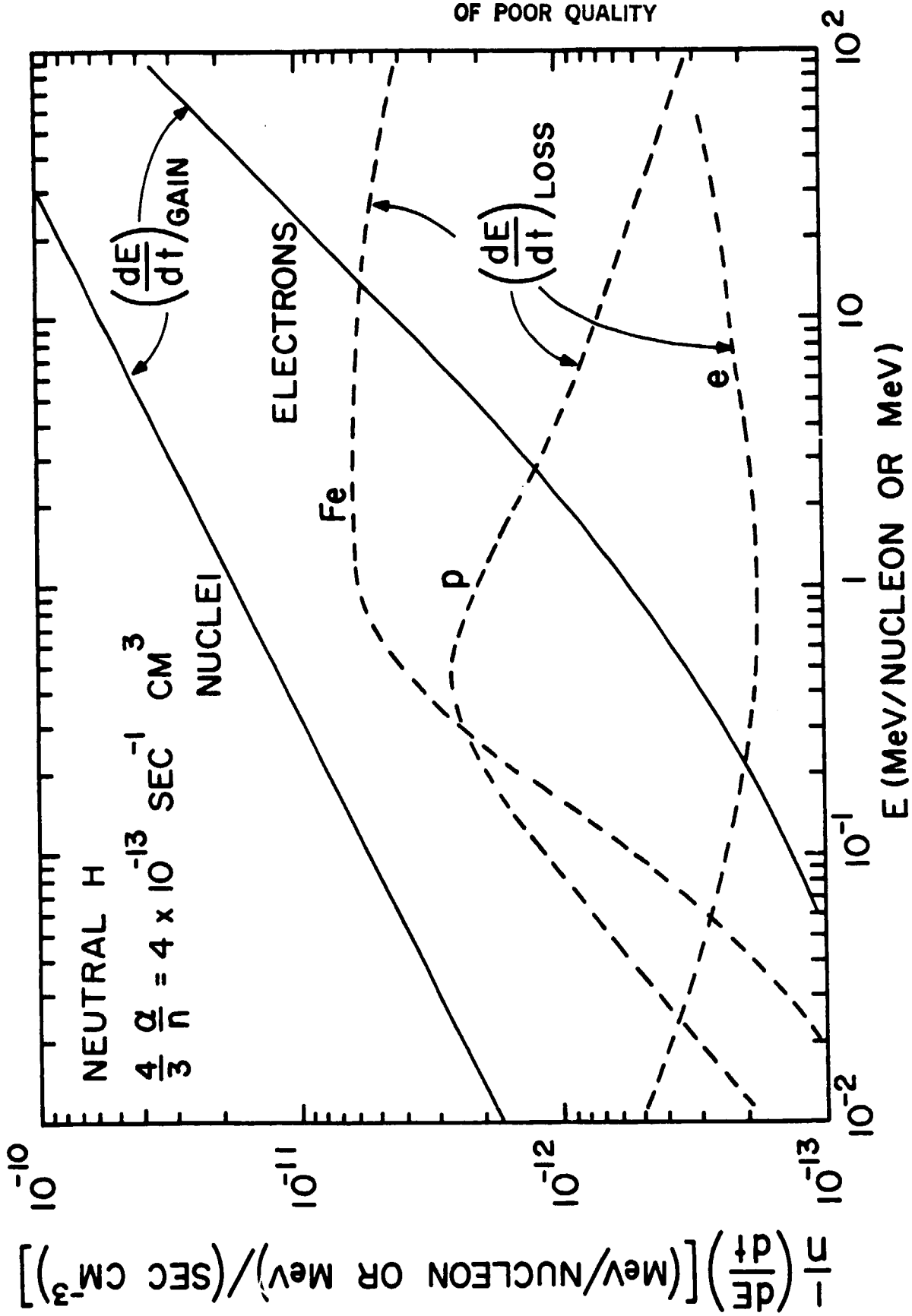

Figure 6

ORIGINAL PAGE IS
OF POOR QUALITY

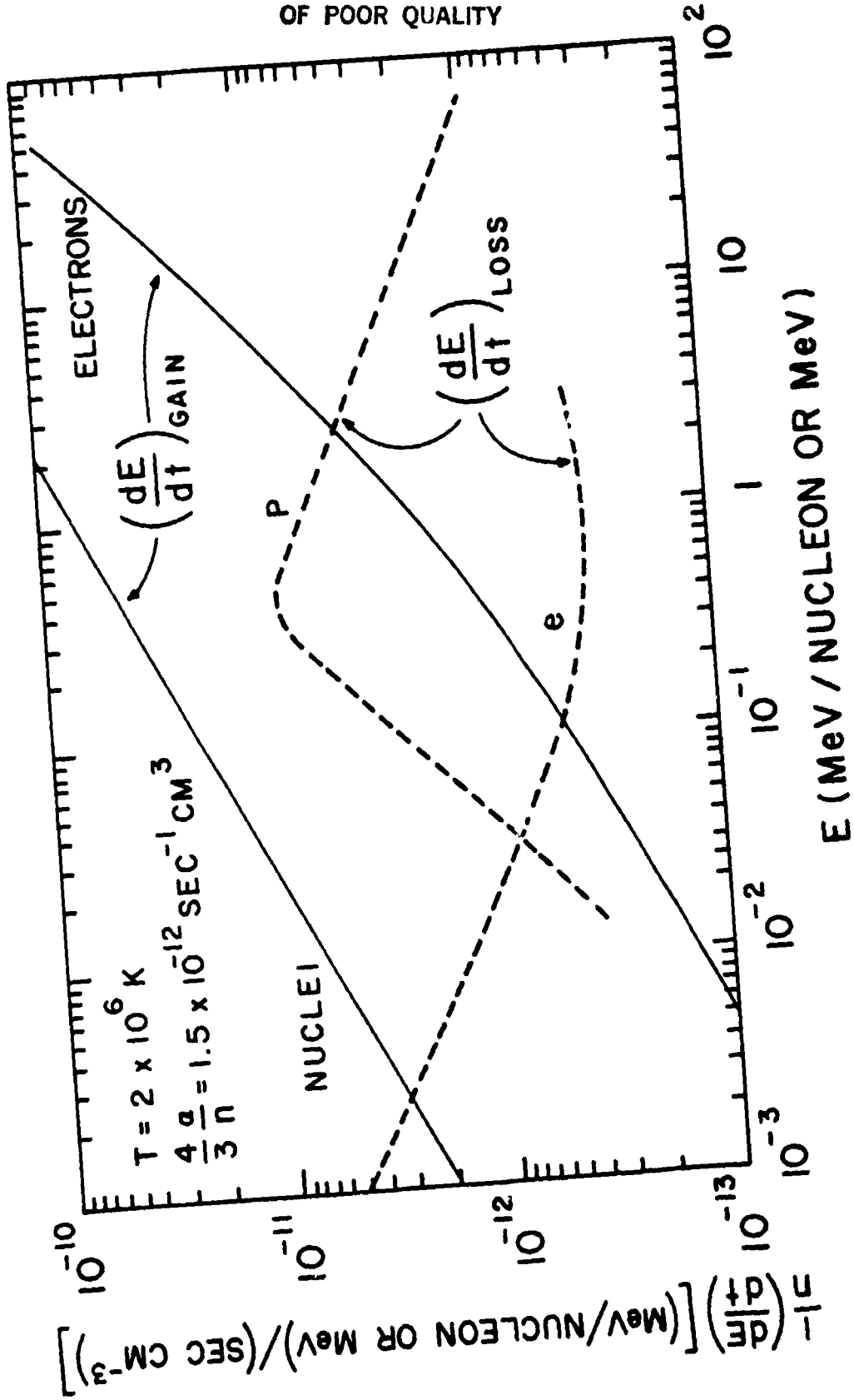

Figure 7

ORIGINAL PAGE IS
OF POOR QUALITY

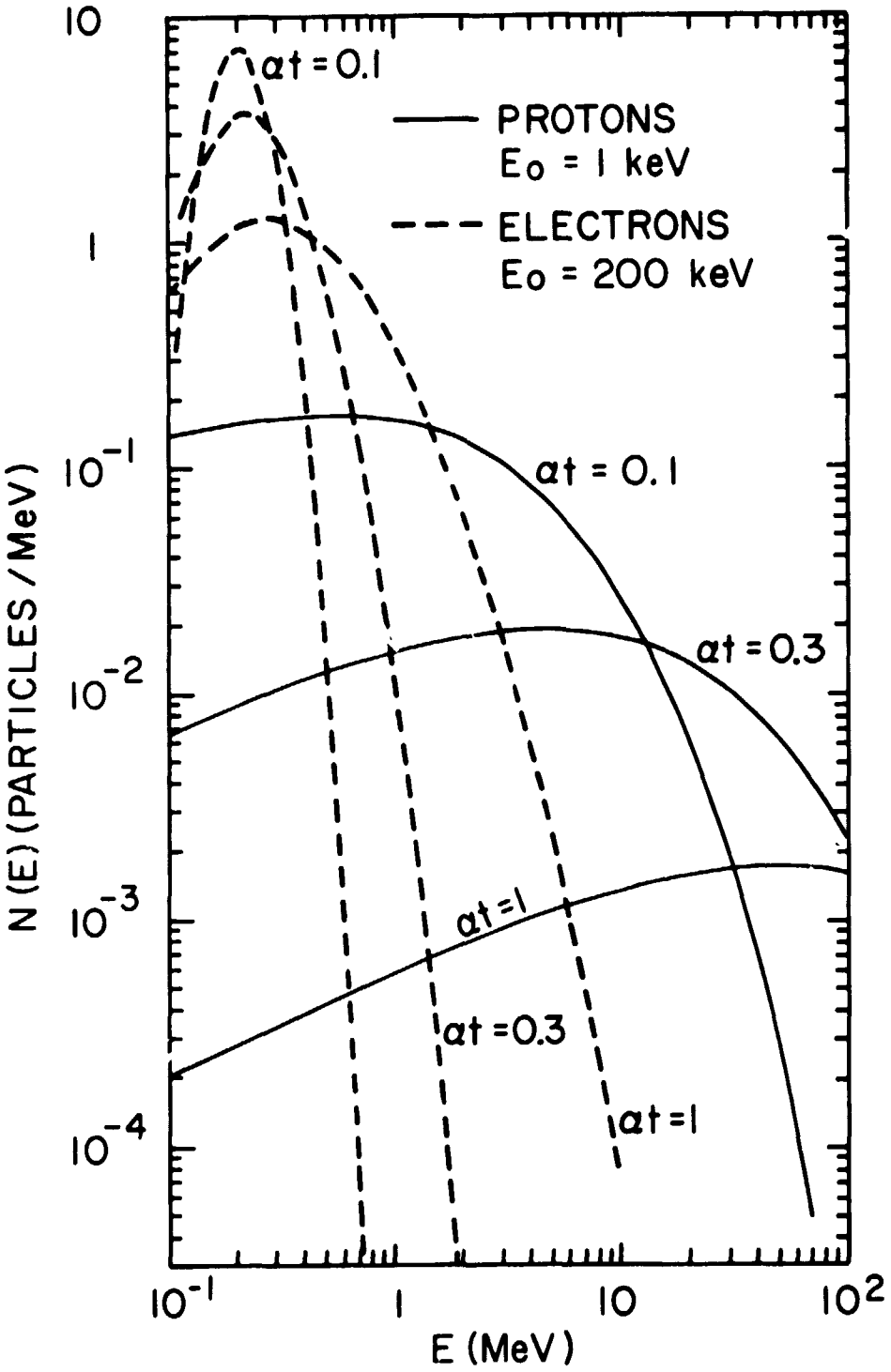

Figure 8

ORIGINAL PAGE IS
OF POOR QUALITY

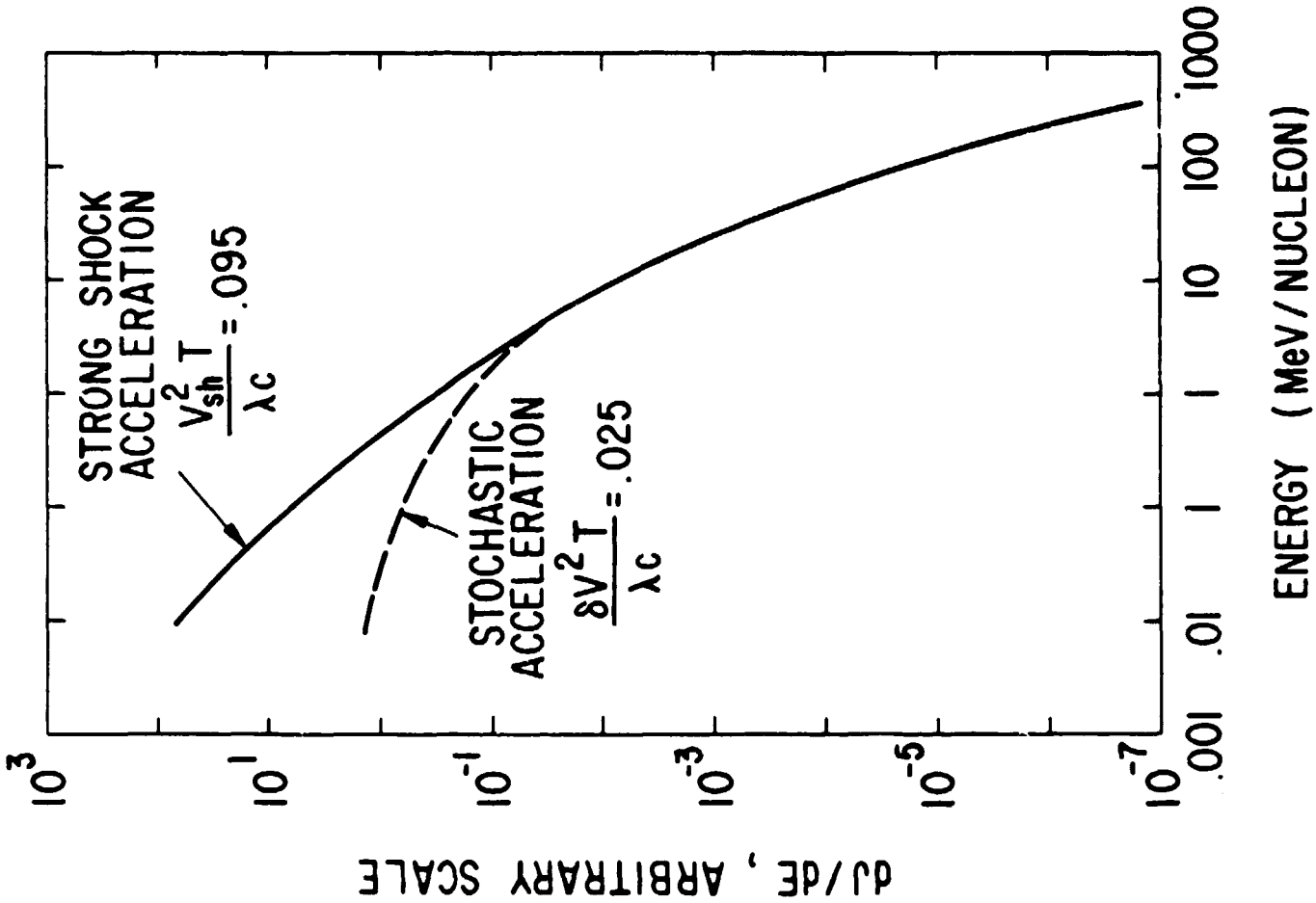

Figure 9

ORIGINAL PAGE IS
OF POOR QUALITY

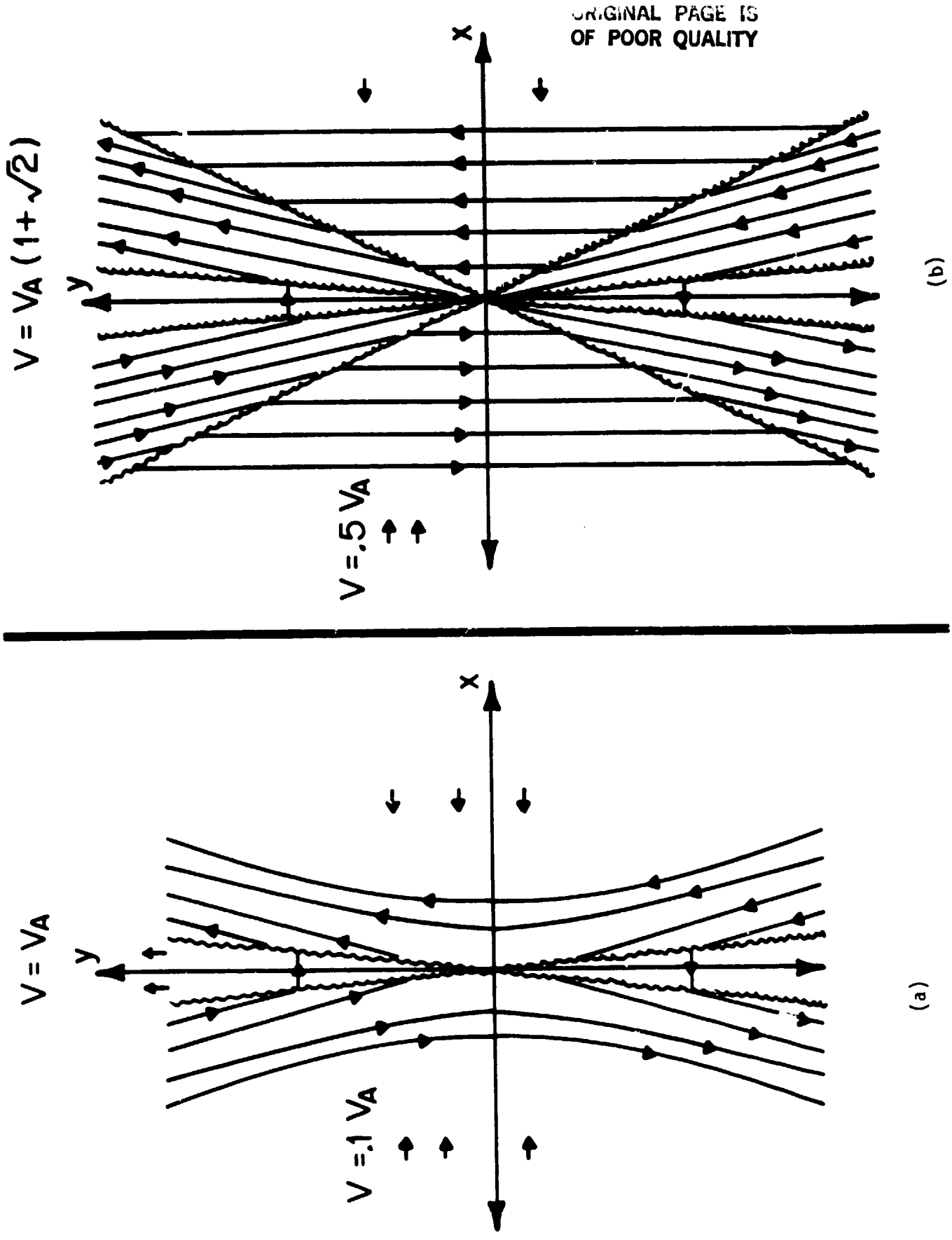

Figure 10

ORIGINAL PAGE IS
OF POOR QUALITY

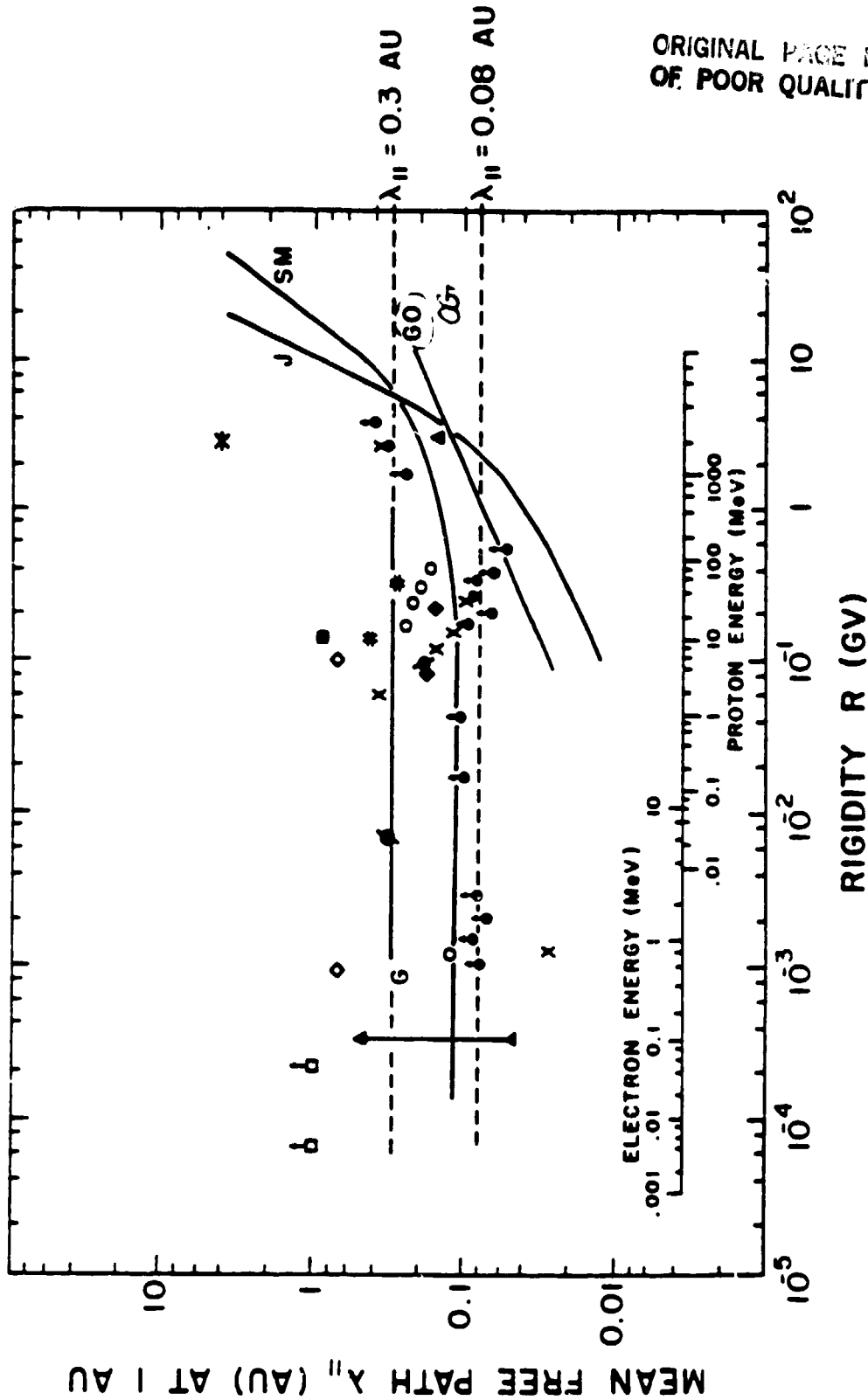

Figure 11

ORIGINAL PAGE IS
OF POOR QUALITY

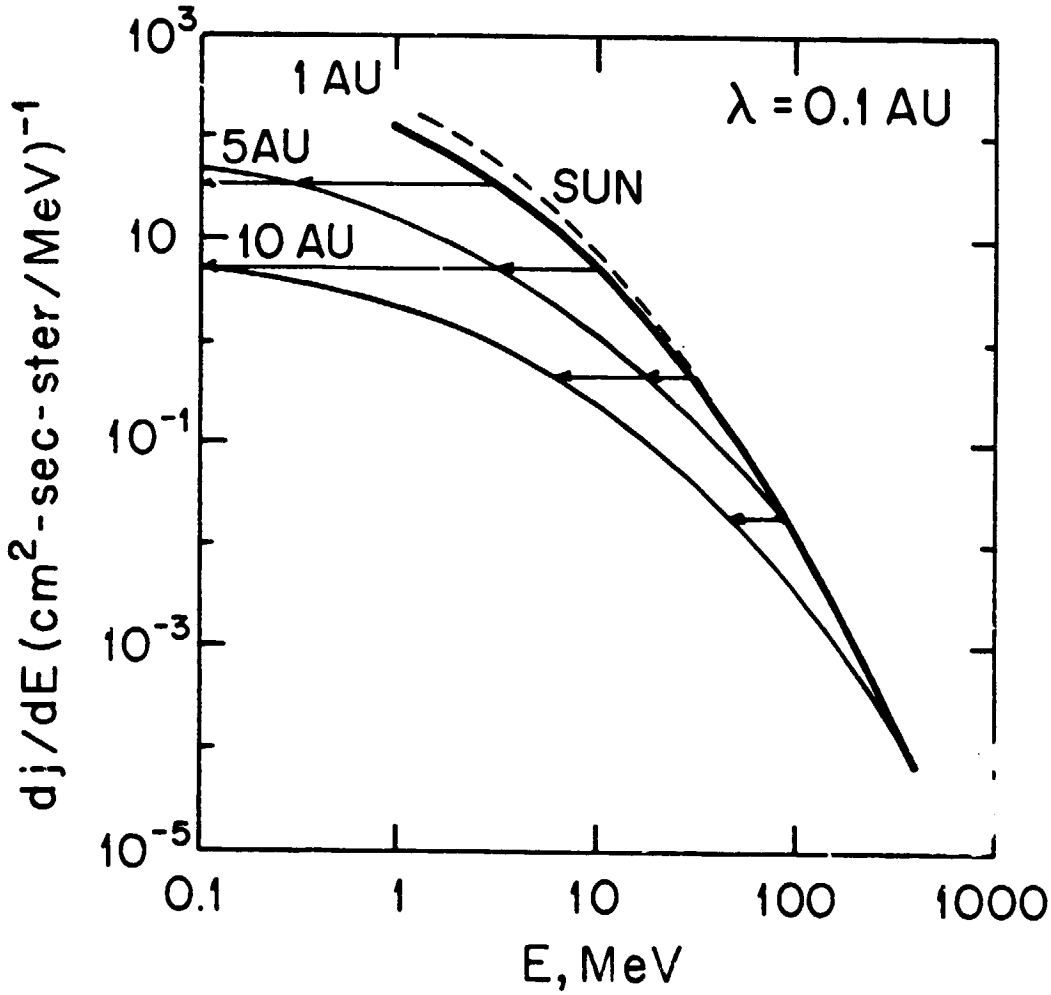

Figure 12